The effect of grafted neuroectodermal stem cells on injured spinal motoneurons following ventral root avulsion and reimplantation: insights into the molecular mechanism

Ph.D. thesis

Krisztián Pajer MSc.

Szeged

2014

The effect of grafted neuroectodermal stem cells on injured spinal motoneurons following ventral root avulsion and reimplantation: insights into the molecular mechanism

Ph.D. thesis

Krisztián Pajer MSc.

Laboratory of Neural Regeneration, Department of Anatomy, Histology and Embryology, Faculty of Medicine, University of Szeged

Supervisor: Prof. Dr. Antal Nógrádi

Szeged

2014

Original papers related to this thesis

I. Pajenda G, **Pajer K**, Márton G, Hegyi P, Redl H, Nógrádi A. Rescue of injured motoneurones by grafted neuroectodermal stem cells: Effect of the location of graft.
Restor Neurol Neurosci. 2013 Jan 1;31(3):263-74. doi: 10.3233/RNN-120294.
Impact factor: 4,179

II. **Pajer K,** Feichtinger GA, Márton G, Sabitzer S, Klein D, Redl H, Nógrádi A. Cytokine signaling by grafted neuroectodermal stem cells rescues motoneurons destined to die.
Exp Neurol. 2014 Jun 5;261C:180-189. Impact factor: 4,617 (2013)

Table of contents

Summary

Avulsion of one or more ventral roots from the spinal cord leads to the death of the majority of affected motoneurons. This process is due to a cascade of events involving activation of astrocytes and microglial cells and the excessive amounts of excitotoxic glutamate release in the injured cord. The aim of the present study was to analyse and compare the therapeutic potential of transplanted NE-GFP-4C murine neuroectodermal cells applied in topically different transplantation paradigms and determine the factors responsible for the motoneuron-rescuing effect.

The lumbar 4 (L4) ventral root of Sprague-Dawley rats was avulsed and reimplanted ventrolaterally into the injured cord. Neuroectodermal stem cells were injected immediately following avulsion injury into the L4 segment, into the reimplanted ventral root or were placed in fibrin clot around the reimplanted root. Three months after the primary surgery the L4 motoneuron pool was retrogradely labelled with Fast Blue and the numbers of reinnervating motoneurons were determined. Expression of various factors expected to prevent motoneuron death in the grafted cord was determined by PCR and immunohistochemistry in short term experiments.

Animals that received intraspinal stem cell grafts have 70% of their L4 motoneurons regenerated into the vacated endoneural sheaths of the reimplanted root. Morphological reinnervation was accompanied by significant functional recovery. Intraradicular neural stem cell grafting (transplantation into the reimplanted root) resulted in good morphological and functional reinnervation, while both negative controls and animals with perineural stem cell treatment showed poor motor recovery.

Stem cell grafts produced the modulatory cytokines IL-1-alpha, IL-6, IL-10, TNF-alpha and MIP-1-alpha, but no neurotrophic factors. The neurons and astrocytes in the ventral horn of grafted animals also produced IL-6 and MIP-1-alpha. The infusion of function-blocking antibodies against all cytokines into the grafted cords completely abolished their motoneuron-rescuing effect, while neutralization of only IL-10 suggested its strong effectivity as concerns motoneuron survival and a milder effect on reinnervation.

In this study we have provided evidence that significant numbers of motoneurons can be rescued both by intraradicular and intraspinal stem cell grafting. The pro-inflammatory and anti-inflammatory cytokines selectively secreted by grafted stem cells act in concert to save motoneurons and to promote reinnervation of the target muscles.

Introduction

Morphology of spinal motoneurons

The cell bodies of spinal motoneurons lie in lamina IX in the Rexed of ventral horn (Rexed, 1954; Rexed, 1952; Jankowska and Lundberg, 1981; Schomburg, 1990). Motoneurons form four separate columns in the human cord: the ventromedial, the ventrolateral, the dorsolateral and the central column. (Romanes, 1964). Spinal motoneurons have larger soma diameter than most other nerve cells in the spinal cord. The α-motoneurons have the largest soma in the spinal cord ranging between 50 and 70 μm. The axons of α-motoneurons are the longest in the mammalian body and innervate extrafusal muscle fibers. The other type of motoneurons is the γ-motoneuron, also called fusimotor neurons innervates intrafusal muscle fibers within the muscle spindle. The soma diameter of γ-motoneurons ranges between 20 and 40 μm. The ß-motoneurons constitute a third distinct category of motoneurons that innervate intrafusal fibers of muscle spindles with collaterals to extrafusal fibers.

The spinal motoneurons are multipolar neurons with several dendrites. The average α-motoneuron has 10-12 dendrites and the stem diameter of dendrites varies between 0.5 and 19 μm (Cullheim *et al.*, 1987a, 1987b). Dendrites typically show a binary manner. One dendrite has two daughters and each dendrite tends to form 12-14 terminal branches. The dendrites of γ-motoneurons show similar dendritic patterns as α-motoneurons but the dendrite branching is simpler and dendritic tree is smaller (Lagerbäck *et al.*, 1981a, 1981b). The dendrites of motoneurons usually show transversally or longitudinally orientated patterns and form dendritic bundles. The motoneurons that lie in the ventromedial column, form vertical and longitudinal branches, whereas dendrites of motoneurons in the central and ventrolateral columns form transversally and longitudinally placed dendritic bundles. On the other hand, motoneurons in the dorsolateral columns rather have radial orientation (Scheibel and Scheibel 1966a, 1966b). This arrangement of dendrites contributes to a precise control of movement and connection of segmental afferents.

The spinal motoneuron has generally one axon giving off 1-5 axon collaterals before leaving the central nervous system (Cullheim and Kellerth, 1978). The first is the recurrent collateral that projects back to the motoneuron and modifies the activity of the cell. The motor axon is well myelinated in the peripheral nervous system. When the axon of the motoneuron enters

the skeletal muscle, they loose the myelin sheath and the terminal fibres run along the surface of the muscle fibres and finally form neuromuscular junctions. The motorneuron and the skeletal muscle fibers innervated by its axon is called collectively „the motor unit" (Cullheim and Kellerth, 1987a, 1987b). Groups of motor units work together to regulate the contraction of a muscle.

Reaction of motoneurons to ventral root avulsion

Adult motoneurons and their processes undergo reversible degenerative changes after an injury inflicting the axon far from the cell body, without loss of the affected motoneuron pool. On the other hand, axonal injury close to the cell body of the motoneuron results in severe changes which may eventually lead to death of motoneurons. Typical injuries affecting the initial part of the motor axon are most frequently avulsion injuries of the ventral roots. Therefore it is generally concluded that ventral root avulsion injuries are likely to result in motoneuron loss (Nógrádi and Vrbová, 1996; Koliatsos *et al.*, 1994).

Morphological changes of motoneurons after ventral root avulsion

Morphological changes of damaged motoneurons are initiated within few days following ventral root avulsion. The cell body of the motoneurons becomes swollen and the nucleus migrates toward the periphery of cells. Nissl (tigroid) bodies, first described by Franz Nissl (1894) and by Mihály Lenhossék (1895) are multilayered sheets of the rough endoplasmatic reticulum with attached ribosomes (Johnston and Sears, 1989). Following avulsion or axotomy this complex brakes up into several small units and tigroid bodies appear to dissolve. This process is known as chromatolysis (Nissl, 1894; Lenhossék, 1895).

Neuronal injury results in the change of mRNA and protein synthesis, too. Tubulin, actin and the regeneration-associated protein GAP-43 mRNA levels increase after axotomy but expression of other proteins such as neurofilament proteins decreases (Tetzlaff *et al.*, 1988).

Dendrites are normally covered with numerous synaptic endings. Damage to the axon induces retraction of dendrites and to loss of many synaptic contacts on the dendrites of motoneurons. During and after regeneration and muscle reinnervation the motoneuron dendrites regain their dendritic area, but the pattern of dendritic arborization remains altered (Brännström *et al.*, 1992).

Motoneurons may develop regenerating axons following ventral root avulsion. The origin of the newly developed axon could be the cell body or the dendrite, in this case, the new axon is called “dendraxon” (Lindå *et al.*, 1985). Axons from cell body are able to extend for a long distance within the gray matter (Havton and Kellerth, 1987). These aberrant axons usually show abnormal projection patterns within the grey and white matter and they express growth-associated protein GAP-43, store choline acetyltransferase (ChAT) and form bouton-like swellings (Havton and Kellerth, 1987).

Glutamate-mediated cell death after ventral root avulsion

Ventral root injury of the spinal motoneurons induces biochemical cascades resulting in glutamate-mediated excitotoxic events (Mills *et al.*, 2001a). Glutamate is an excitatory neurotransmitter in the central nervous system (CNS). Glutamate release is normally followed by rapid re-uptake from the synaptic cleft. Glutamate receptors can be divided into two groups: ionotropic N-methyl-D-aspartate (NMDA) and AMPA/kainate receptors or metobotropic receptors (Ha *et al.*, 2002; Mills *et al.*, 2001b). Metabotropic glutamate receptors are G-protein-coupled and their injury-dependent activation induces numerous intracellular cascades that have long-lasting effect after injury (Mills *et al.*, 2001b). Injury upregulates the subtypes of NMDA and AMPA/kainate receptors which play a key role in glutamate-mediated excitoxic cell death (Beattie *et al.*, 2010). Activation of NMDA receptors leads to the influx of Ca^{2+} ions into neurons. Increased cytoplasmatic concentration of Ca^{2+} ions induces various secondary processes resulting in cell death (Terro, 1998). Interestingly, spinal neurons are more vulnerable to AMPA/kainate than to NMDA toxicity while cortical neurons are rather vulnerable to NMDA toxicity (Regan, 1996).

Role of astrocytes and microglia after injury

Astrocytes

Asrocytes are located in the CNS and their morphology depends on their location but their function and roles are similar in all regions of the CNS. Two forms of astrocytes occur in the CNS: the fibrillary (mainly present in the white matter) and the protoplasmic astrocyte (confined to the grey matter). Not only the levels of excitatory neurotransmitter glutamate in the synaptic clefts are modulated by them but they influence neuronal calcium, potassium

levels within extracellular space after action potential, too (Parpura *et al.*, 1994; Walz *et al.*, 1984). In addition astrocytes play key role in the maintance of the optimal pH of CNS via converting carbon dioxide to water and proton (Hertz *et al.*, 1988). Astrocytic' endfeet take part of the blood brain barrier (Vise *et al.*, 1975). The deletion of functional GFAP gene gives rise to abnormal blood-brain-barrier function.

After a CNS injury the morphology, the phenotypic characteristics and the protein expression pattern of the astrocytes are altered. These responses contribute to glial scar and chemical barrier formation. The expression of S100β and GFAP proteins is increased following CNS trauma but other proteins such as many of developmental markers including nestin and vimentin are started to be expressed by astrocytes (Vijayan *et al.*, 1990; Corvino *et al.*, 2003; Clarke *et al.*, 1994). Moreover, the levels of inhibitory extracellular matrix molecules such as ephrins and chondroitin sulphate proteoglycans are increased by astrocytes (Morgenstern *et al.*, 2002). Those astrocytes that undergo these changes are called reactive astrocytes. The reactive astrocytes can derive from astrocytes that are present at the time of the injury or from progenitor cells that are found around the central canal or the subpial region of spinal cord (Beattie *et al.*, 1997). The glial scar formation is the other negative contribution of reactive astrocytes to the unsuccessful regeneration. The glial scar forms a physical barrier around the injury so the axons are not able to regenerate through this barrier (Beattie *et al.*, 1997).

However, atrocytes have several actions that contribute to the endogenous repair and neuroprotection of the CNS following injury. The astrocytes express various neurotrophic factors that probably contribute to survival of the damaged neurons (Ikeda *et al.*, 2001, Krenz and Weaver, 2000). Furthermore, they express glial glutamate transporter (GLT-1) that is able to reduce excitotoxic cell death after injury (Rothstein *et al.*, 1996). Although they produce several molecules that inhibit growth of neurites, they also express extracellular matrix molecules that are supportive to axon growth (Costa *et al.*, 2002).

Microglia

Microglia give around 15-20% of all glia cells of CNS. They derive from bone marrow precursor cells and form the first line of defense. The activation status of the microglia can be divided into three classes: resting microglia, activated microglia and phagocytic microglia (Streit *et al.*, 1988). In the healthy CNS microglia cells are in resting status. However, the

resting microglia exhibit very extensive activity. They extend and retract their fine processes throughout the neuropil to survey the local environment (Nimmerjahn *et al.*, 2005). In addition to this they have many other roles in the CNS. During embryogenesis they phagocytose apoptotic neurons and promote the death of developing neurons (Bessis *et al.*, 2007). The microglia act as a regulator of adult neurogenesis in the subventricular zone and dentate gyrus (Battista *et al.*, 2006; Walton *et al.*, 2006).

Damage to cells of CNS results in the release of ATP, glutamate and changes of extracellular ion content. Microglia cells are sensitive for these molecules and transform from resting status to amoeboid form and start to express various cytokines and chemokines. They undergo rapid ploriferation and begin to upregulate major histocompatibility complex (MHC) antigens and other antigens that make them as antigen presenting cells (Wang *et al.*, 2002; Hickey and Kimura, 1988). Upon injury, microglia can be divided into two groups, M1 and M2 cells. In general, the M1 state is a defensive one. The activation of classical M1 pathway leads to the production of interleukin-1-beta (IL-1β), interleukin-18 (IL-18), tumor necrosis factor alpha (TNF-alpha), proteases and chemokines. Activation of M1 status is rapid and persistent (Kigerl *et al.*, 2009). Nitric oxyde synthase is the most widely used marker to detect M1 activation. In contrast, M2 is an alternative form that is responsible for anti-inflammatory responses as it produces the anti-inflammatory cytokine IL-10. The activation of M2 is associated with encapsulation of parasites, matrix deposition and tissue remodeling. Mannose receptor and arginase 1 facilitate to detect M2 activation.

Some studies have shown that microglia remove the presynaptic element from the cell body and dendrites then their processes enwrap the cell body (Trapp *et al.*, 2007; Blinzinger and Kreutzberg, 1968). These observations suggest that microglia may be involved in synatpic stripping following peripheral nerve injury.

The microglial cells are able to produce numerous neurotrophins, neuroprotective factors and anti-inflammatory proteins, including IL-1 receptor antagonist (IL-1ra), IL-10, nerve growth factor (NGF), transfroming growth factor β (TGF-β), brain derived neurotrophic factors (BDNF) (Aloisi *et al.*, 1999; Liu *et al.*, 1998; Kiefer *et al.*, 1998). The expression of these factors improves the survival of injured motoneuron and regeneration. However, it is not fully understood why activated microglia produce cytotoxic pro-inflammatory proteins and neurotrophic factors at the same time.

Effects of neurotrophic factors, pro- and anti-inflammatory cytokines on injured motoneurons

Neurotrophic factors, pro- and anti-inflammatory proteins are critical mediators of the post-traumatic reactions. Below a list of factors is provided that have been analyzed in our study and might be acting on injured motoneurons. We investigated the expression of a number of neurotrophic and immune factors known to play a role in the inflammatory and regenerative events following spinal cord injury and cell damage.

Neurotrophic factors regulate motoneuron survival and appeare to be able to induce endogenous regenerative processes. The nerve growth family includes several members such as BDNF, neurotrophin-3 (NT-3) and neurotrophin-4 (NT-4). Members of this family act through two types of receptors, the receptor tyrosine kinases Trk and the low affinity nerve growth factor receptor p75. The activation of Trk receptors leads to the activatation of the survival pathways, Ras-ERK and PI3K/pAkt. Numerous studies have shown that endogenous BDNF induces sprouting and axonal growth following peripheral nerve lesion and promotes axonal regeneration of adult rat spinal motoneurons (Streppel *et al.*, 2002; Zhang *et al.*, 2000; Novikov *et al.*, 1997). On the other hand, administration of exogenous BDNF protects motoneurons following ventral root avulsion (Zhang *et al.*, 2000; Novikov *et al.*, 1997). Receptor for NT-3 (Trk-C) is present in adult motoneurons but it is down-regulated following axotomy or avulsion injury (Hammarberg *et al.*, 2000). In vitro studies have also shown that NT-4 is a survival factor for motoneurons (Henderson *et al.*, 1993). Exogenous application of NT-4 in NT-4 knockout mice was able to induce improved regeneration compared to untreated control (English *et al.*, 2005).

The other potent factor in the transforming growth factor beta family is the glia derived neurotrophic factor (GDNF) that is able to induce motoneuron regeneration after ventral root avulsion (Pajenda *et al.*, 2014). GDNF binds to the specific GDNF family receptor α (GFR α) proteins and the common transmembrane co-receptor c-ret (Airaksinen and Saarma, 2002). The receptor complex signal through the RET receptor tyrosine kinase leads to improved cell survival, proliferation and differentiation (Sariola and Saarma, 2003). Both receptors are upregulated in motoneurons following ventral root avulsion, thereby GDNF is able to induce motoneuron survival after avulsion injury.

The neuropoietic family includes interleukin-6 (IL-6), also known as a pro-inflammatory protein. IL-6 is expressed by inflammatory cells, astrocytes, microglia and neurons. IL-6 interacts with the signal-transducing β-subunit of IL-6 receptor complex (gp130) and protects cerebellar granule neurons against NMDA-induced apoptosis, mediated by the JAK-STAT3 and the PI3K-Akt signaling pathways (Liu *et al.*, 2011) However in motoneurons gp130 expression is downregulated following avulsion injury. Therefore this cytokine has no direct effect on injured motoneurons (Hammarberg *et al.*, 2000).

Interleukin-10 (IL-10) is regarded as an anti-inflammatory cytokine. In glutamate induced neurotoxicity IL-10 binds to the IL-10 receptor (IL-10R) that leads to the activation of janus-associated kinases/signal transducers and transcription factors and phosphatidylinositol 3-kinase-AKT pathways and enhances expression of antiapoptotoic peptides Bcl-2 and Bcl X_L (Zhou *et al.*, 2009a). In lateral hemisection model overexpression of IL-10 resulted in increased neuronal survival in the anterior quadrant of the spinal cord and improved motor function (Zhou *et al.*, 2009b). IL-10 might be a good candidate to prevent motoneuron death following ventral root avulsion injury.

Interleukin-1 (IL-1-alpha and IL-1-beta) is a highly inflammatory cytokine. IL-1-alpha and IL-1-beta can act on the IL-1 receptor (IL-1R) and induce various intracellular signaling. Following CNS trauma activated glial cells are the major source of IL-1 that is rapidly released. Several studies have shown that IL-1 forms a common link between various intracellular cascades and contributes to the cell death in CNS diseases (Rothwell and Luheshi, 2000). However, others have provided evidence that IL-1 imparts neuroprotective effect against excitotoxicity in a concentration-dependent manner (Carlson *et al.*, 1999).

TNF-alpha is produced by glial cells in the brain, and contributes to the pathogenesis of inflammatory neurodegenerative diseases (Tran *et al.*, 2008; Chao *et al.*, 1995). Interestingly, TNF-alpha can have both pro- and anti-inflammatory outcomes. Probably TNF-alpha alone causes only minor inflammatory changes but its expression in combination with other cytokines can induce neurotoxicity (Chao *et al.*, 1995). On the other hand, others studies have reported that administration of TNF-alpha protects cultured neurons against an excitotoxic death (Carlson, *et al.*, 1998). It has been suggested that the differential effect of TNF-alpha is receptor dependent: TNF-alpha contributes to the protection of neurons against chronic NMDA-mediated excitotoxic death via activation of p55/TNFRI, but not p75/TNFRII

(Carlson, *et al.*, 1998).

MIP-1-alpha, also known as Chemokine (C-C motif) ligand 3 (CCL3) belongs to the family of chemotactic cytokines (chemokines). MIP-1-alpha induces the synthesis and release of other pro-inflammatory cytokines such as IL-1, IL-6 and TNF-alpha from fibroblasts and macrophages in the peripheral immune system (Maurer and Stebut, 2004). MIP-1-alpha can act through G-protein–coupled receptors and control the cytokine profiles in the injured CNS (Mennicken *et al.*, 1999). Mechanical injury, neuroinflammatory processes and neurodegenerative processes induce chemokine actions via upregulated chemokine receptors.

Experimental therapeutic approaches to prevent motoneuron loss occuring after ventral root avulsion

Ventral root avulsion is an axon injury occuring very close to the cell body. One of the possible ways to rescue injured motoneurons is the reimplantation of the avulsed ventral root or peripheral nerve graft implantation. These permissive conduits provide a trophic support and regenerative pathways via vacated endoneural sheaths for the axon injured motoneurons (Li and Raisman, 1994). Reimplantation of ventral root induces motoneuron survival and injured motoneurons' axons are able to reinnervate the reinserted root (Nógrádi and Vrbová, 1996). However in the case of delayed surgical repair the proximal nerve stump retracts and reimplantation is not possible anymore.

Regenerating axons of motoneurons have two possible routes to reinnervate the implanted nerve graft or ventral root. One is that the regenerating motor axons grow along the pia matter and reach the nerve graft (Risling *et al.*, 1992). The other way is that the motoneurons send their axons through a non-permissive environment and the axons grow straight into the peripheral nerve graft (Carlstedt, 1997). It is well known that a number of factors promote not only the motoneuron survival but the axon regeneration, too. Schwann cells release various trophic factors that present an attractive force for axons and these factors play key role in guiding of axons. Two phenotypes (motor and sensory) of Schwann cells have been identified by Höke and his colleagues (Höke at al., 2006). They express trophic factors differentially upon denervation and reinnervation. Another study by Su *et al.* (2013) has confirmed that following reimplantation of avulsed ventral root induces better motoneuron survival and regeneration than a peripheral nerve graft.

It has been shown, that reimplantion of an avulsed root combined with the treatment of the anti-excitotoxic compound riluzole (2-amino-6-trifluoromethoxybenzothiazole) rescued the majority of the injured motoneurons otherwise destined to die (Nógrádi and Vrbová 2001; Nógrádi *et al.*, 2007; Pintér *et al.*, 2010). Earlier studies have shown that riluzole not only prevented the death of the damaged lumbar and cervical motoneurons but also enabled them to regenerate their axons into the reimplanted ventral root and thus provided functional reinnervation for the denervated limb musculature (Nógrádi *et al.*, 2007, Pintér *et al.*, 2010). Another way to rescue injured motoneurons is the combination of intrathecal GDNF and intraperitoneal riluzole application which improve motoneuron survival and induce a number of axons to regenerate into the reimplanted ventral root (Bergerot *et al.*, 2004).

Recent attempts other than therapeutic efforts to reduce excitotoxicity to the damaged motoneurons have been made to rescue adult motoneurons following avulsion injury, including therapy only with only neurotrophic factors (Blits *et al.*, 2004; Eggers *et al.*, 2008; Novikov *et al.*, 1995). In these studies neurotrophic factors were applied near the denervated motoneuron pool. Treated animals showed an increased survival of motoneurons, but motoneurons failed to extend their axons into the reimplanted root and did not produce functional recovery of the hind limbs.

A recent strategy to rescue injured motoneuron following ventral root avulsion is progenitor and stem cell therapy (Su *et al.*, 2009). In generally there are a great number of stem and progenitor cells that can be used in the CNS to induce neuronal survival, axon regeneration or replace missing cells. While many of these cell treatment strategies apply stem cells that bring little or not significant improvement in morphological restoration and in function, there are few therapeutic approaches where the applied cells are proven to be safe and effective at long term (Bottai *et al.*, 2010).

Fate of NE-GFP-4C cells

In our studies we used a p53-deficient clonal neuroectodermal stem cell line subclone (NE-GFP-4C) derived from E9 mouse embryonic forebrain (Schlett *et al.*, 1997). These cells were identified geno- and phenotypically and expressed the green fluorescent protein (GFP) (Schlett and Madarász, 1997). Under normal conditions the NE-GFP-4C cells were able to divide continuously and express several non-differentiated neural stem cells markers without

showing any neuronal differentiation. In the presence of all-trans retinoic acid the NE-GFP-4C cells started to differentiate into neurons and astrocytes and showed well-defined characteristics of neuronal and glial physiology and morphology (Herbert *et al.*, 2002; Tárnok *et al.*, 2002; Schlett and Madarász, 1997). If NE-GFP-4C cells were maintained in contact or noncontact perinatal astrocyte co-cultures, immature astrocytes enhanced the differentiation of these neural stem cells to neurons and astrocytes. (Környei *et al.*, 2005). Transplantation of NE-GFP-4C cells into newborn or postnatal intact brains induced tumor-like formation and the grafted cells did not migrate and differentiate in the host tissue (Demeter *et al.*, 2004). In contrast to newborn or postnatal grafting, NE-GFP-4C cells were able to survive and proliferate for long time without forming any tumor-like aggregates in the embryonic or adult brain (Demeter *et al.*, 2004). Furthermore, these neural stem cells were able to survive and proliferate in the freeze-lesioned adult mouse brain cortices, although differentiation of these cells was not detected under these conditions (Zádori *et al.*, 2011). Application of hypoperfusion-induced hypoxia in the lesioned mouse cortices induced differentiation of grafted neural stem cells into neurons and reduced the proliferation of these cells (Zádori *et al.*, 2011).

Aims of the study

In this study we intended

1) to test whether grafted neuroectodermal stem cells are able to rescue injured motoneurons and promote the regeneration of their axons,

2) to study the effect and capacity of stem cells grafted at various locations within and in the vicinity of the injured spinal cord segment, and

3) to determine the factors which are responsible for the motoneuron-rescuing effect of grafted stem cells.

Material and methods

Maintenance of NE-GFP-4C stem cells

The clonal neuroectodermal stem cells (NE-GFP-4C cells, a gift from Dr. E. Madarász, Institute of Experimental Medicine, Hungarian Academy of Sciences, Hungary; also available from ATCC, No. CRL-2926 and Dr. Ernő Duda, Biological Research Centre, Hungarian Academy of Science, Hungary) were originally isolated from 9-day-old forebrain vesicles of embryos of transgenic mice lacking the tumour suppressor gene p53, and were made to produce eGFP as described previously. NE-GFP-4C stem cells were maintained on nuncloned petri dishes (VWR International, Debrecen, Hungary) in High-glucose Dulbecco Modified Essential Medium (H-DMEM, Sigma, Hungary) supplemented with 10% foetal calf serum (Gibco) at 37 °C and 5% CO_2. Floating cells appeared after 3 days and were passaged every 2 days, using trypsin digestion and mechanical dissociation. The medium was changed daily. All cell cultures underwent at least two, but no more than five passages before transplantation.

Ventral root avulsion-reimplantation and various transplantation paradigms

All together 184 female Sprague-Dawley rats (Animal Research Laboratories, Himberg, Austria, and Animal Facilities at the Faculty of Medicine, University of Szeged, weighing 180-220 g body weight) were used. Animals survived for 2, 5, 10, 14 or 16 days or for 1, 3 or 6 months. Out of these, ninety-four animals participated in retrograde labelling and immunohistochemistry, 48 operated and 9 intact animals in semiquantitative and qPCR studies, 8 animals in tension recording studies, 15 animals in functional blocking experiments and 16 in CatWalk semiautomated gait analysis.

All the operations were carried out under deep ketamine-xylazine anaesthesia (ketamine hydrochloride: 90 mg/kg body weight, Ketavet, Pharmacia & Upjohn Co.; xylazine: 5 mg/kg body weight, Rompun, Bayer Co.) and sterile precautions. To maintain the body temperature at 37.0±0.5°C, the rats were kept on a heating pad during the surgery. Laminectomy was performed at the level of T13–L1 vertebrae, the dura was opened and the left L4 ventral root was pulled out leaving the dorsal roots intact. Then the cut end of the ventral root was inserted into the lateral part of the spinal cord. To avoid damage to the cord, a small hole was created on the lateral surface of the cord, and the avulsed root was inserted into the hole using a watchmaker's forceps (Dumont, Switzerland, No. 5). Special care was taken to avoid damage

to the cord, including its motoneuron pool, or to the reimplanted root (Fig. 1A-B). The control experiments involved either intact animals or rats whose L4 root was avulsed and reimplanted without a stem cell graft (AR group, Fig. 1A). In group 2 animals (ARG-PR group) the reimplanted root was surrounded by 3×10^5 stem cells applied in a loose fibrin matrix (Baxter Ltd, Vienna, periradicular grafting of stem cells, Fig. 1B). Group 3 animals (intraradicularly grafted rats, ARG-IR) received 3 injections of stem cells (5×10^4 each) along a 3 mm length of the reimplanted root (Fig. 1C). The proximal injection was applied immediately at the re-established ventral root-spinal cord junction zone, the second and the third injections were applied approx 1.5 mm from the junction zone and from the second injection site, respectively. Animals in group 4 (intraspinal grafting of stem cells, ARG group) had 3×10^5 stem cells injected into the caudal part of the L4 segment (Fig. 1D). The spinal cord was covered with the remaining dura, the wound was closed and the animals were allowed to recover (Nógrádi and Vrbová, 1996; 2001). Animals survived for 5 or 10 days or for 3 months. No immunosupressive treatment was applied.

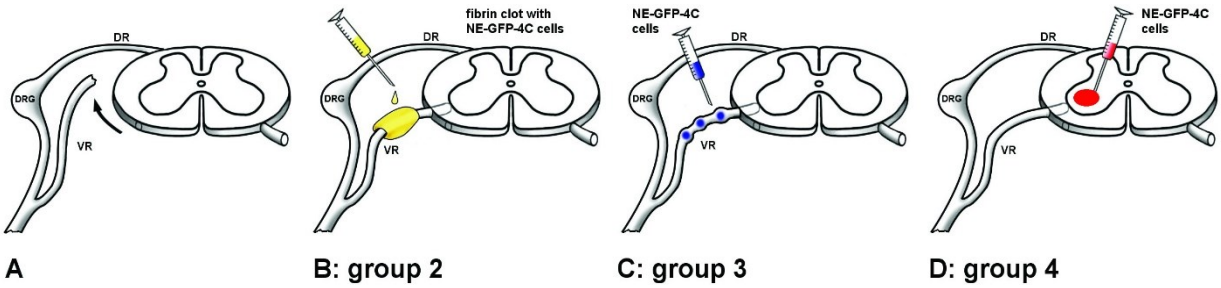

Figure 1. Schematic drawing depicting the various experimental paradigms

Three experimental surgical approaches are shown: (A) After avulsion of the L4 ventral root 3×10^5 stem cells were mixed in fibrin clot and applied around the reimplanted root (B, group 2, ARG-PR). In other experimental groups stem cells were injected at three locations into the reimplanted root (5×10^4 cells at each site, group 3, in C, ARG-IR) or 3×10^5 cells were grafted into the spinal cord along with reimplantation of the avulsed root (D, group 4, ARG).

In the other experiments animals had $5x10^4$, 1x, 2x or $3x10^5$ stem cells were injected into the caudal part of segment L4. All experiments were carried out with the approval of the Animal Protocol Review Board of City Government of Vienna and with that of the Committee for

Animal Experiments, University of Szeged and rules regarding the care and use of animals for experimental procedures were followed. All the procedures were carried out according to the Helsinki Declaration on Animal Rights. Adequate care was taken to minimize pain and discomfort.

Retrograde labelling

Three months after the surgery, the animals were deeply anaesthetized as described above. On the operated side, the ventral ramus of the left L4 spinal nerve was sectioned and the proximal stump of the nerve was covered with a few Fast Blue (FB) crystals. Four days after the application of this fluorescent dye, the animals were reanaesthetized and were perfused transcardially with 4% paraformaldehyde in 0.1 mol/l phosphate buffer (pH=7.4).

Semiquantitative PCR, list of tested factors

Spinal cords were homogenized twice for 10 sec in 600 µl RLT buffer + ß-MeETOH (Qiagen GmbH, Hilden, Germany) with a MagNaLyser (Roche, Rotkreuz, Switzerland) at a speed of 5,500 rpm with an intermediate pause for 5 min on ice. The resulting lysates were incubated on ice and subjected to centrifugation at 13,000 rpm for 1 min at room temperature. The lysates were subsequently used for RNA extraction with the QIAcube robot system (Qiagen) and the RNeasy Mini Kit protocol for large samples (Qiagen). After DNaseI treatment (Turbo DNA-free Kit, Ambion, Austin, TX, USA), the RNA was measured both qualitatively and quantitatively with an Agilent 2100 Bioanalyzer (Agilent, Vienna, Austria). An RNA Lab chip (Agilent RNA 6000 Nano Reagents) was used to determine the RNA integrity number. cDNA was synthetized with a High-Capacity Reverse Transcription Kit (Applied Biosystems, Foster City, CA, USA) The appropriate 5' and 3' primers for PCR were designed manually and then tested with AmplifX software (Mac version, Supplementary Table 1). The appropriate conditions (e.g. annealing temperatures) for each cytokine, chemokine and neurotrophic factor were first established by gradient-PCR, using a positive control consisting of mouse and rat embryo tissue or injured mouse and rat spinal cord. To establish the quantification in the linear range, different cycle numbers were used depending on the target genes: IL-1-alpha, IL-1-beta, TGF-beta, MIP-1-alpha and PDGF-alpha were amplified at 30 cycles, while hypoxanthine-guanine phosphoribosyltransferase (HPRT), the other cytokines and the

neurotrophic factors were amplified at 35 cycles. The RT-PCR results for the cytokines, chemokines and neurotrophic factors at each time point (2, 5, 10 and 14 days after surgery) were expressed as a proportion of the corresponding intensity value of the HPRT product (densitometric measurement).

List of genes studied in injured and grafted spinal cords		
Factor	RefSeq accession	Sequence (5' to 3') sense
BDNF	NM_007540	CTGGTGCAGAAAAGCAACAA
GDNF	NM_010275	ACATAGGGGAACTGTGCAGG
IL-1-alpha	NM_010554	AGACCATCCAACCCAGATCA
IL-1-beta	NM_008361	GACCTTCCAGGATGAGGACA
IL-6	NM_031168	GAGGAGACTTCACAGAGGA
IL-10	NM_010548	ATGGCCCAGAAATCAAGG
NT-3	NM_001164035	TGCCGGAAGACTCTCTCAAT
NT-4/5	NM_198190	AAGGATGGGATCAGGGAAAG
PDGF-alpha	NM_008808	GAGATACCCCGGGAGTTGAT
PDGF-beta	NM_011057	CCAGATCTCTCGGAACCTCA
PTN	NM_008973	TGTGAGGGCTTAAAACACCC
MCP-1	NM_011333	TCACCTGCTGCTACTCATTCAC
MCSF	NM_007778	GAAAGTGAAAGTTTGCCTCGGTGCTCT
MIP-1-alpha	NM_011337	GGGCATATGGCTTCAGACACCAGA
TGF-beta	NM_011577	AGAACACCCACTTTTGGATCTCAG
TNF-alpha	NM_013693	TCAGCGAGGACAGCAAG

Table 1. List of genes studied in injured and grafted spinal cords

Tissue staining and laser capture microdissection (LCM), quality control of RNA

All tissues were quick-frozen in liquid nitrogen and stored at -80 °C until further use. LCM was performed with the Veritas instrument (Arcturus, CA, USA), equipped with a cutting laser (349 nm) to cut a narrower outline around the region of interest and a capture laser (810 nm) to capture the entire region within the outline. The procedure has been described previously[30]. In brief, 10 µm thick tissue sections were cut on a Leica CryoCut Jung CM1800 cryostat (Leica Instruments, Nußloch, Germany) by using an RNAse-free technique, mounted onto special membrane slides (Molecular Machines & Industries, Glattbrugg, Switzerland) and stained immediately after cutting with the HistoGene LCM Frozen Section Staining kit (MDS Analytical Technologies, Ismaning, Germany). The sections were then cleared in xylene for 5 min and either used directly for microdissection or stored at -80 °C until further

use. Regions of interest were cut and captured into CapSure Macro LCM caps (MDS, Ismaning, Germany). The laser power setting ranged from 60 to 80 mW, and the pulse settings from 1,700 to 2,500 µsec. Spot size was determined prior to microdissection and adapted to each tissue type. During an LCM session, dissection of an area of approximately 200,000 – 250,000 µm² (~ 1,000 cells) led to amplifiable results in the subsequent qPCR. The remaining tissue on the slide was used for RNA quality measurement using the RNeasy Micro Kit (Qiagen) for RNA isolation. The protocol including the DNaseI treatment was carried out directly on the columns. After the overall procedures, the RNA quality measurements were analysed with the Agilent 2100 Bioanalyzer applying the RNA 6000 pico Lab chip (Agilent).

Quantitative RT-PCR (qRT-PCR)

A two-step qRT-PCR was performed with the High-Capacity Reverse Transcription Kit (Applied Biosystems) for cDNA synthesis and adjacent qPCR measurements were performed with the Power Sybr Green Kit (Applied Biosystems). The cDNA was synthetized on a StepOnePlus cycler (Applied Biosystems) and the qPCR was performed on the 7900HT Sequence Detection System (Applied Biosystems). The expression levels of different genes of interest (MIP-1-alpha, TNF-alpha, IL-1-alpha, IL-6 and IL-10) were measured by qRT-PCR. The relative expression levels of these genes were calculated in relation to two different house-keeping genes (glyceraldehyde-3-phosphate-dehydrogenase [GAPDH] and HPRT) using the ddCt method. As the data obtained with the use of GAPDH appeared to be more reliable, these are presented here.

The primers of the assays used in this study were designed through the use of the Primer Express software version 2.0 (Applied Biosystems). The house-keeping gene assays were designed to detect mouse and rat mRNA transcripts and were based on mRNA alignments (SECentral software, Cary, NC, USA) using the following reference genes: mouse BC082592 and rat X02231 sequences for GAPDH, and mouse NM_013556 and rat BC098629 for the HPRT assay. In order to exclude the detection of DNA, the primers were located on different exons. The primers used for the GAPDH assay were: sense: 5'- GGC CTT CCG TGT TCC TAC C -3´ and antisense: 5'- GCC TGC TTC ACC ACC TTC TT - 3´; and for HPRT: sense: 5'- GGT GGA GAT GAT CTC TCA ACT TTA AC -3´ and antisense: 5'- TGT ATC CAA CAC TTC GAG AGG TCC -3´.

The genes of interest were designed to detect mouse and rat sequences, too. The primers used for the different assays were: MIP: sense: 5'- TGC CCT TGC TGT TCT TCT C - 3' and antisense: 5'- ATT CTT GGA CCC AGG TCT CTT - 3'; PDGF: sense: 5' – TAG ACT CCG TAG GGG CTG A – 5' and antisense: CAA TAC TTC TCT TCC TGC GAA TGG - 5'; TNFa: sense: 3'- ACT GAA CTT CGG GGT GAT CG - 5' and antisense: 5'- TTG AAG AGA ACC TGG GAG TAG A -3'; IL-1: sense: 5'- AGA CCA TCC AAC CCA GAT CA - 3' and antisense: 5'- CGG TCT CAC TAC CTG TGA TG -3'; IL10: sense: 5'- ATG GCC CAG AAA TCA AGG-3' and antisense: 5'- CGA GGT TTT CCA AGG AGT TG -3'; IL6: sense: TTC CCT ACT TCA CAA GTC CGG-3' and antisense: 5'- TAC AAT CAG AAT TGC CAT TGC A-3'; PDGFnew: sense: 5'- CTG GCT CGA AGT CAG ATC CAC -3' and antisense: 5'- GGG CTC TCA GAC TTG TCT CCA -3'.

All assays were validated by using standard dilution series of a positive control over at least 4 log decades. The reaction efficiency was calculated from each standard curve via the formula: E: $10^{-1/slope}$ -1.

Immunohistochemistry

For spinal cords 25 μm transverse sections were cut on a cryostat (Leica CM 1850, Leica GmbH, Nussloch, Germany) and mounted onto gelatin-coated glass slides. Non-specific binding sites were subsequently blocked with 3% normal donkey, goat or horse serum. Primary antibodies were incubated overnight at 4 ^{o}C, washed, and then incubated with fluorescent-conjugated secondary antibodies for 1 h at room temperature. The following primary antibodies were used: anti-mouse IL-1-alpha, IL-6, TNF-alpha and MIP-1-alpha (1:50, all from R&D Systems, Minneapolis, MN, USA), anti-mouse IL-10 (1:400, Biolegend, San Diego, CA, USA), mouse anti-GFAP (1:100 Santa Cruz Biotechnology, Inc, CA, USA), polyclonal chicken anti-green fluorescent protein (GFP) (1:2,000, Chemicon), biotinylated Griffonia (Bandeira) simplicifolia lectin B_4 (GSA-B_4, 1:200, Vector Labs, Burlingame, CA, USA), anti-mouse/rat IL-1-alpha, IL-6, IL-10, TNF-alpha and MIP-1-alpha (1:200, all from Abbiotec, San Diego, CA, USA), goat anti-choline acetyltransferase (1:200, Millipore, Billerica, MA, USA), anti-mouse M6 (mouse-specific neuron marker, 1:400 DSHB, IA, USA), anti-mouse M2 (mouse-specific astrocyte marker, 1:400, DSHB), anti-mouse MOG (mouse-specific oligodendrocyte marker, 1:50, R&D Systems, Minneapolis, MN), anti-

neurofilament 200kD (NF200, Abcam Ltd, 1:200, Cambridge, UK) and anti-SSEA-1 (stage-specific mouse embryonic antigen-1, 1:400, DSHB). Secondary antibodies were used as follows: Alexa Fluor 594 donkey anti-rat, Alexa Fluor 546 goat anti-rabbit, Alexa Fluor 546 donkey anti-goat, Alexa Fluor 488 goat anti-chicken, Alexa Fluor 488 goat anti-rabbit, horse biotinylated anti-goat IgG (H+L) and horse biotinylated anti-mouse IgG (H+L). Immunohistochemistry and lectin histochemistry were visualized with either the streptavidin Alexa Fluor 546 conjugate or the streptavidin Alexa Fluor 488 conjugate (1:400, Invitrogen). To validate TNF-alpha and IL-1-alpha immunohistochemistry, Mg^3HeLa cells transfected with TNF-alpha plasmid (a kind gift from Ernő Duda, at the Biological Research Centre, Szeged, Hungary) and rat testis were used, respectively.

Fluorescence signals were detected in an Olympus BX50 epifluorescence microscope equipped with a DP70 digital camera (Olympus Ltd, Tokyo, Japan). Confocal microscopic images were obtained by using an Olympus FluoView® FV10i compact confocal microscope.

Function-blocking antibody experiments

Adult female rats (n=5 in each set of experiments) were deeply anaesthetized and the avulsion-reimplantation of the L4 ventral root and transplantation of $3x10^5$ NE-GFP-4C cells were performed as described above. A mini-osmotic pump (Alzet Osmotic Pumps, Cupertino, CA, USA; type 1002, 100 µl volume) filled with a mixture of function-blocking antibodies against MIP-1-alpha, IL-1a, IL-6, TNF-alpha (4 µg/ml working concentration, all from R&D Systems, Minneapolis, MN, USA) and IL-10 (Biolegend, San Diego, CA, USA) was placed subcutaneously in the dorsal region. All antibodies were specific to mouse epitopes only. A silicone tube (Degania Silicone Ltd, Kibbutz Degania, Israel, 0.3 mm in internal diameter) extended from the mini-pump to the spinal cord and its distal end was inserted into the cord at the site of grafting. The tube was fixed to the surrounding musculature with 8-0 sutures (Ethilon) to avoid moving in or out of the spinal cord. In another set of experiments osmotic pumps filled with IL-10 antibody only (4 µg/ml working concentration) were used. Control animals received pumps filled with physiological saline only. The pumps were removed 2 weeks after the operation. The animals survived for 3 months and were then processed for motoneuron counts and histological analyses.

Cell counts

The number of retrogradely labelled cells was determined on 25 µm thick serial cryostat sections. To avoid double counting of neurons present in consecutive sections, the retrogradely labelled neurons were mapped with the aid of an Olympus (Olympus Ltd, Tokyo, Japan) drawing tube, and their locations were compared with those of the labelled neurons in the previous section. All sections from the L4 motoneuron pool were used (Nógrádi *et al.*, 2007).

Quantification of astrocyte and microglia density

To assess the density of GFAP-positive astrocytes and GSA-B_4-positive microglia in injured and grafted ventral horns, we photographed injured, grafted and contralateral intact horns for each rat at a 10-fold primary magnification, using a Olympus BX50 epifluorescence microscope at a distance of 0.5, 1, 1.5, and 2 mm rostral and caudal to the reimplanted ventral root (n=5/group). With ImageJ Software (NIH), we measured the relative densities of GFAP and GSA-B4 immunoreactivity in the ventral horns. The background/autofluorescence of unstained samples as reference intensity was then subtracted from the intensity of injured grafted and of intact ventral horns in order to determine the final density. The GFAP and GSA-B4 intensity of the injured and grafted ventral horns was then divided by that of the contralateral intact ventral horns. We additionally performed automatic thresholding for each image by using NIH ImageJ software to determine the threshold for the specific signal. After the threshold had been set, the density above the threshold was quantified.

Analysis of the locomotion pattern – the CatWalk semiautomated gait analysis

For determination and analysis of the parameters of the hindlimb movement pattern in the different experimental paradigms, the 'CatWalk' automated quantitative gait analysis system was used (Noldus Ltd, Wageningen, The Netherlands, version 7). This computer-assisted method of locomotor analysis made it possible to quantify several gait parameters, including the duration and speed of different phases of the step cycle and print areas detected during locomotion. The following parameters were taken into account during the analysis:

the print area (expressed in mm^2): the total floor area contacted by the paw during the stance phase,

the print intensity (expressed in arbitrary units): the mean pressure exerted by one individual paw during the floor contact;
the print width (expressed in mm): the parameters describing the width of the print area,
the stance duration (expressed in s): the stance duration is the time of the stance phase,
the swing speed (expressed in m/s): swing speed is computed from the swing duration and the stride length.
the base of support of the hind limbs (BOS, expressed in mm): The base of support of the hind limbs is the distance between the two hind paws of the rat (Hammers *et al*., 2001; Hammers *et al.*, 2006)

Muscle tension recording

The animals selected for tension recording (n=4 in both the control and the intraspinal group) were anaesthetized with ketamine-xylazine at the end of the 3-month survival period and the tibialis anterior and extensor digitorum longus muscles of both the reinnervated and the contralateral control hindlimb were prepared for tension recording. These muscles were chosen for tension recording because the motoneurons innervating them are mainly found in spinal segment L4 (Lowrie *et al.,* 1984). The muscles of the contralateral leg were considered to be suitable controls because their tension increased with age in a similar way to that for the muscles of the normal, unoperated animals. The distal tendons were dissected free and attached to strain gauges, and the exposed parts of the muscles were kept moist with Krebs' saline solution. Isometric contractions were then elicited from the muscles by stimulating the ventral ramus of the L4 spinal nerve with bipolar electrodes. The length of each muscle was adjusted so as to produce the maximum twitch tension. Single twitch and tetanic (40-100 Hz) contractions were displayed and recorded on a computer; all the additional recording hardware and software were developed by Supertech Ltd (Pécs, Hungary, system “Kellényi”). Maximum tetanic tension was achieved at a stimulation frequency of about 100 Hz. An estimate of the numbers of motor axons supplying the muscles was obtained by stimulating the L4 spinal nerve with stimuli of increasing intensity and recording the stepwise increments of twitch contractions.

Statistical analysis

The non-parametric Mann-Whitney U test and the One way ANOVA test and Two way ANOVA test with Tukey's all pairwise multiple comparison procedures were used to compare the data on the groups. Values are reported throughout the thesis as means ± S.E.M and $p < 0.05$ was considered significant.

Results

General observations, functional improvement, the CatWalk gait analysis system in the different transplantation paradigms

The aim of the next experiments was to compare the therapeutic potential of 3 x 10^5 transplanted NE-GFP-4C cells applied in topically different transplantation paradigms (see Fig. 1). Behavioral analysis was started two weeks after surgery and the first signs of functional recovery were observed 4-5 weeks after reimplantation of the ventral root. Control (AR) and ARG-PR (periradicular grafting) animals showed minimal improvement, i.e. their affected hind limb was placed laterally with minimal dorsiflexion of the ankle joint and the spreading reflex was minimal or completely missing. In contrast, animals that received grafts into the L4 ventral root (ARG-IR, intraradicular grafting) or into the spinal cord (ARG) developed a movement pattern closely similar to that of the intact hind limb. Movements of the ankle joint, especially dorsiflexion was extensive and toe spreading was present. Quantitative gait analysis obtained from the CatWalk automated gait analysis system showed that the earliest differences in functional recovery between these groups appear from week 6 and these differences became significant by week 8 to 10 (Fig. 2). Improved footprint parameters (print area, intensity, print width, stance duration) in the groups ARG-IR and ARG indicated an improved stability of foot placing, while parameters characteristic of the step cycle (swing speed and base of support of the hind limbs) showed improved movement pattern in group ARG-IR and ARG animals (Fig. 2), too. Interestingly, animals that received intraspinal or intraradicular stem cell grafts did not show significantly different gait parameters.

Retrograde labelling studies, number of reinnervating motoneurons in various grafting protocols

The number of retrogradely labelled motoneurons, i.e those motoneurones that were able to send their axons into the vacated endoneural sheaths of the reimplanted ventral root correlated with the functional data. Control animals that had their ventral root avulsed and reimplanted but received no stem cell graft (AR group) had very few reinnervating cells (42 ± 10 SEM, n = 5). Similarly, in the spinal cords of ARG-PR animals which received a periradicular stem

cell graft, more retrogradely labelled motoneurons were found (65 ± 2.5 SEM, n = 5), without significant difference between these two groups (Fig. 3). On the other hand, grafting of NE-GFP-4C cells into the reimplanted root (ARG-IR, n = 5) or into the spinal cord (ARG, n = 5) produced similarly good results: the numbers of reinnervating cells were 671 ± 26 SEM and 711 ± 14 SEM, respectively (Fig. 3). It is noted, that the reinnervating cells in these two groups comprised 58% and 61% of the intact L4 motoneuron pool (1158 ± 14 SEM, n = 4), suggesting a very effective rescuing mechanism.

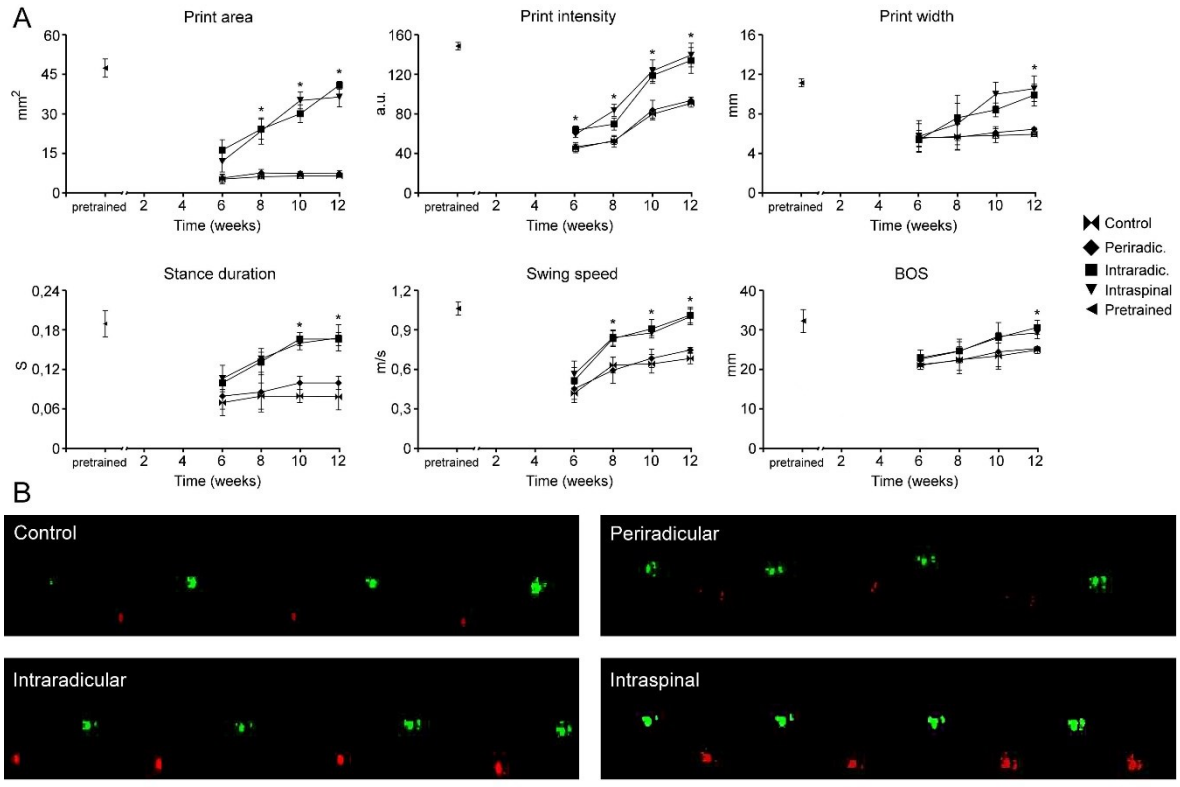

Figure 2. Results of the CatWalk automated gait analysis

The gait analysis revealed significant differences between the AR and ARG-PR groups and ARG-IR and ARG groups. The earliest significant differences in functional recovery between these groups appeared from week 8 in case of some parameters. Both the parameters indicating improved stability of foot placing (print area, intensity, print width, stance duration) and that of improved step cycle (swing speed and base of support of the hind limbs) suggested significant functional reinnervation in group ARG-IR and ARG animals. Note that the improved parameters of animals in ARG-IR and ARG groups approached the pre-training levels. Asterisks indicate significant differences between groups

AR and ARG-PR and groups ARG-IR and ARG by using the two-way measurement analysis of variance (ANOVA) computed according to Tukey's all pair-wise multiple comparison procedures, $p < 0.05$. The foot prints in the lower panel are taken from individual animals from each experimental group (green prints: intact hind limb, red prints: operated hind limb). Note the recovered print size in the case of intraradicular and intraspinal grafting paradigms.

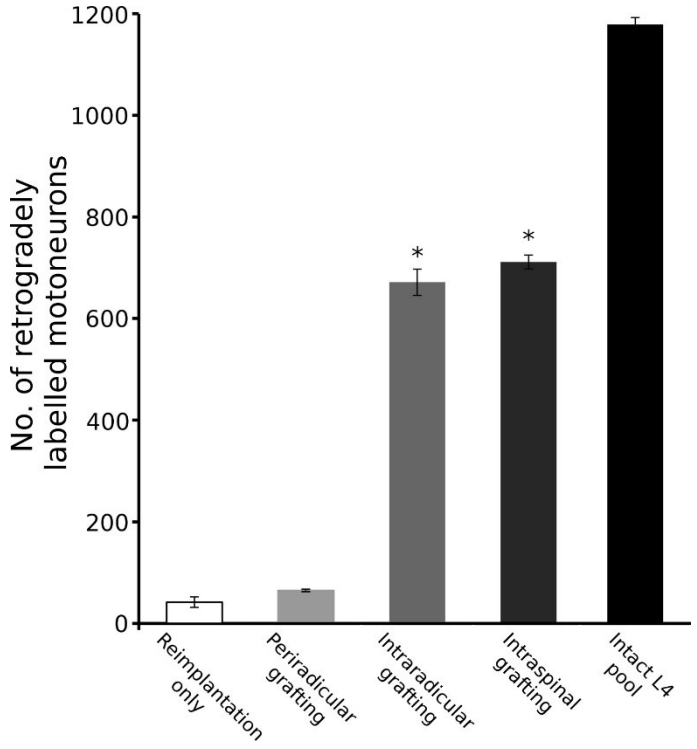

Figure 3. Bar chart showing the results of retrograde labelling studies from the L4 spinal nerve

Transplantation of stem cells into the reimplanted ventral root (ARG-IR) or into the spinal cord (ARG) resulted in equally high numbers of retrogradely labelled motoneurons in the L4 segment (no significant difference was found between these groups). Transplantation of the stem cells around the reimplanted root (ARG-PR) induced as limited reinnervation as reimplantation of the L4 root only (AR, control animals). * = Groups ARG-IR and ARG were significantly different from animals in both the AR and ARG-PR groups, $p < 0.01$, One-way ANOVA.

Differentiation and location of grafted neuroectodermal cells in various experimental groups

The early differentiation and migration of the grafted cells was studied 5 and 10 days after grafting in animals that received stem cells intraradiculary, periradicularly or intraspinally.

Rats that received stem cell grafts embedded in fibrin clots and placed around the reimplanted ventral root (ARG-PR group), formed a well-defined tissue cuff around the reimplanted ventral root 5 days after grafting (Figs. 4A-D). The stem cells expressed the stage-specific embryonic antigen-1 (SSEA-1), an early murine stem cell marker and most of them maintained their GFP expression. However, by 10 days after grafting most of the cells became dispersed and only few of them were found around the reimplanted root (Figs. 5A-B). At this stage of development, these cells expressed the M2 and M6 antigens, characteristic of mouse glial and neuronal phenotypes, respectively, but morphologically they remained rounded, and undifferentiated (Figs. 5A-B, M2 not shown). In the animals that received intraradicular stem cell grafts (ARG-IR), numerous NE-GFP-4C cells were found within the L4 ventral root 5 days after grafting (Figs. 4E-H). The cells formed clusters at the sites of injections and most of them were still able to express GFP. On the other hand, stem cells that expressed SSEA-1 displayed a decreased or faint GFP expression, suggesting that the GFP expression pattern decreases with differentiation. Ten days after grafting we found fewer grafted cells at the sites of microinjections and most of the stem cells expressed SSEA-1 but many of them were already able to differentiate to glial or neuronal phenotypes (M2+ astrocytes and M6+ neurons, Figs. 5D-E). Interestingly, those intraradicularly grafted cells that were placed close to the spinal cord were able to migrate closer to, but not into the injured cord via the reimplanted ventral root and started to differentiate morphologically, too (Figs. 5D-E, M2 not shown). The intraspinal grafts (ARG animals) formed a large cluster of cells that first expressed the SSEA-1 antigen ((Figs. 4I-L) and then further differentiated to M2+ astrocytes and M6+ neurons, respectively (Figs. 6B-E). Five days after grafting mainly SSEA-1+ cells were found in the graft (Fig. 4I and Figs. 6B-B'), whereas by 10 days after grafting the presence of murine astrocytes and neurons was overwhelming (Figs. 6D-E'). During the next few days, the differentiated cells ceased their GFP expression and largely migrated away from the implantation site, leaving there only limited numbers of differentiated cells (16 days survival, n=4, Figs. 6F-G). Numerous stem cell-derived neurons (501±84) and astrocytes

(465±81) settled throughout segment L4 in the following weeks (1 month survival, n=5, Figs. 6H and 6K), while only very few (45±16) oligodendrocytes of graft origin could be detected.

The first signs of axon outgrowth was also observed 10 days after reimplantation in these samples: few regenerating axons visualized by neurofilament (NF-200 kD) immunostaining were seen in the reimplanted root of animals that received intraradicular or intraspinal grafts of stem cells (Fig. 5F and 5I), while such regenerating neurites were infrequently seen in the reimplanted ventral root of animals with periradicularly grafted stem cells (Fig. 5C). Interestingly, several regenerating axons were found in this latter group among the derivatives of stem cells close to the reimplanted root (Fig. 5B).

Three months after grafting in the periradicularly treated animals (ARG-PR group) only few stem cell-derived neurons and astrocytes were sporadically seen along the initial segment of the reimplanted root, typically in the dorsal angle between the reimplanted root and the lateral surface of the spinal cord (Figs. 7A-B). Greater numbers of stem cell-derived neurons and axons were found in the spinal segments of animals with intraradicular grafts (ARG-IR group). These cells were located mainly at the periphery of the root, not in close contact with the regenerated axons (Figs. 7D-E). Interestingly, a number of M2+ astrocytes and M6+ neurons appeared to have migrated into the ventral horn of the damaged L4 segment where these cells were located around the reimplanted root and the reinnervating motoneurons (Figs. 7D-E). Although many cells expressed M2 and M6 antigens on their membranes, only those cells appeared morphologically differentiated which settled in the spinal cord.

The cells that stayed in the reimplanted root remained rounded and appeared morphologically undifferentiated while they expressed murine surface antigens characteristic of mature cells (Fig. 7D). In the spinal cords of animals that received stem cells intraspinally (ARG group), relatively well-differentiated derivatives of stem cells were found, scattered throughout the L4 segment (Fig. 6J and Fig. 7C). The stem cells and their derivatives were rarely seen in contact with the injured motoneurons (Fig. 6I). Three months after grafting, the astrocytes and neurons were still confined nearly exclusively to the injured L4 segment (Fig. 6J). By a survival time of 6 months (n=5) their numbers had decreased critically (Fig. 6K).

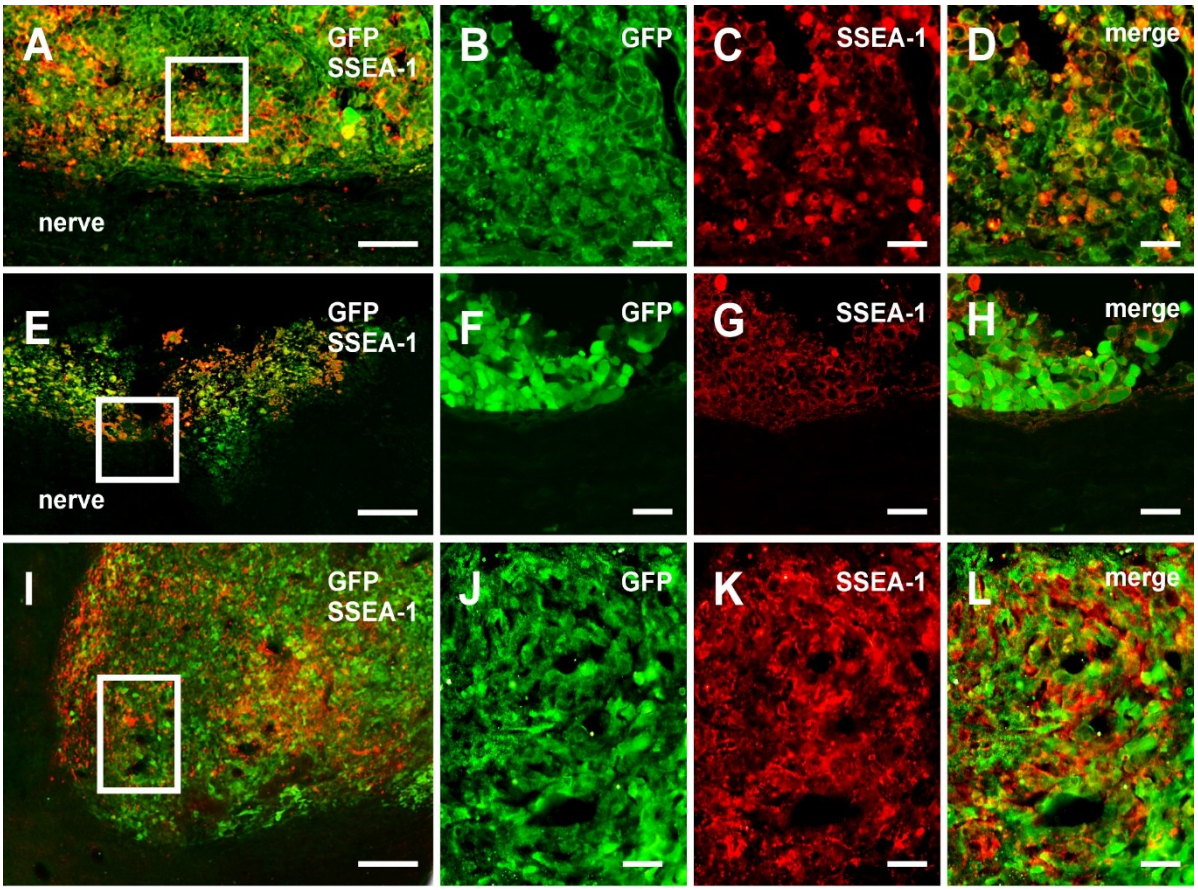

Figure 4. Location and early differentiation of grafted stem cells in various experimental paradigms

A-D shows differentiating NE-GFP-4C cells 5 days after transplantation around the reimplanted ventral root. The cells appear as a tissue mass outside the epineurium. **E-H** displays intraradicularly grafted stem cells just under the connective tissue sheath of the root (not labelled) and **I-L** indicates the location and gene expression pattern of intraspinally grafted stem cells, in both cases 5 days after grafting. Note that many of the grafted GFP+ cells in all experimental paradigm express SSEA-1, a murine stage-specific stem cell marker. **A-H** are confocal images. Note that the confocal images were obtained by the use of various optical thickness settings. Scale bar in **A,E** and **I** = 100 μm, in the rest of the figures = 20 μm.

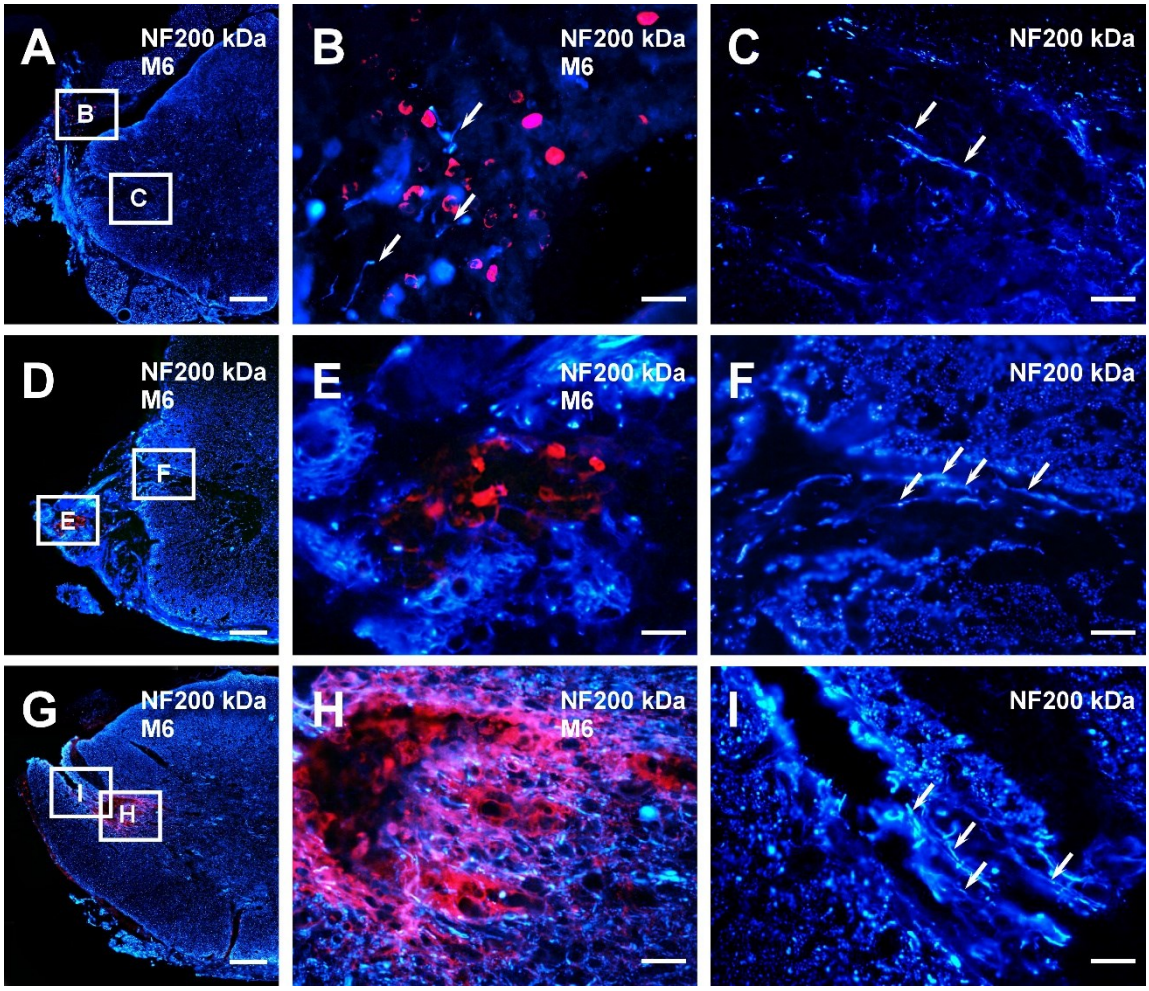

Figure 5. Outgrowth of regenerating axons from the ventral horn of the injured cord into the reimplanted root 10 days after grafting

A shows a hemicord that received a periradicular stem cell graft (ARG-PR group, Neurofilament 200kDa immunohistochemistry - blue). Insets enlarged in **B** and **C** show the location of the M6+ grafted cells (red) within the ventral horn and the few NF200+ regenerating axons (arrows), respectively. Note the few axons (arrows) terminating around the surviving stem cells in **B**. In **D** a section of a spinal cord is displayed with the reimplanted root, into which the stem cells were grafted (NF200 kDa, ARG-IR group). **E** and **F** show the proximal injection site in the reimplanted root (**E**, M6 mouse neuronal marker, red), and the site of reimplantation with numerous regenerating axons (arrows in **F**, NF200 kDa immunohistochemistry). In **G**- to **I** microphotographs taken form intraspinally grafted animals (ARG) are presented. Differentiating (M6 positive) stem cells (red) are located within the cord, at the end of the reimplanted ventral root (**G** and **H**). Numerous NF200kDa+ axons (blue and indicated by arrows) entered the reimplanted root. Scale bar in **A,D** and **G** = 100 μm, in the rest of the figures = 20 μm.

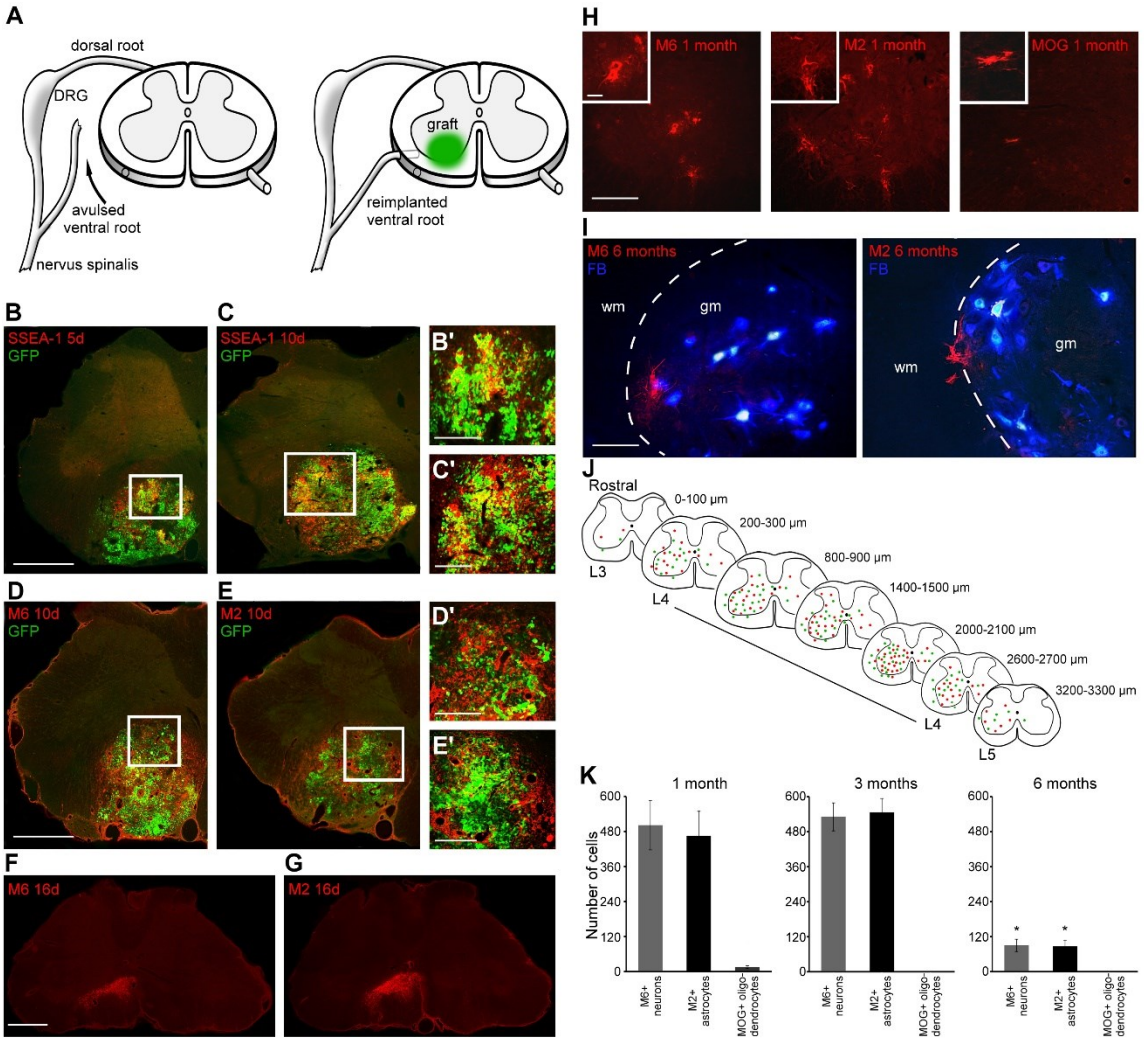

Figure 6. Differentiation and migration of grafted stem cells and their derivatives in the spinal cord

A. Schematic drawing showing the surgical procedure of avulsion, stem cell grafting and reimplantation of the avulsed L4 ventral root (ARG group). **B,C.** Expression of embryonic stem cell marker SSEA-1 by the grafted stem cells 5 and 10 days after transplantation. **D,E.** Initial differentiation of the grafted stem cells to M6+ neurons and M2+ astrocytes, accompanied by the loss of GFP expression. **F,G.** Dispersion of the differentiated stem cells from the site of grafting, where only limited numbers of astrocytes and neurons of graft origin remain. **H.** Numerous M6+ neurons and M2+ astrocytes are present in the cord 1 month after grafting, whereas MOG+ oligodendrocytes are rarely found. **I.** Only a few stem cell-derived neurons and astrocytes, but no oligodendrocytes are located in the host cord 6 months following transplantation. **J.** Distribution of M2+ astrocytes (green dots) and M6+ neurons (red dots) in the injured L4 segment one month following grafting in a representative ARG animal. Each spinal cord cross-section represents a 100 µm thick segment of the

cord. The vast majority of the stem cell-derived cells are located in the affected L4 segment. **K.** The absolute numbers of stem cell-derived neurons, astrocytes and oligodendrocytes are shown at various time points after grafting, n=5. Data are presented as mean +/- S.E.M, $p<0.05$. The one-way ANOVA analysis with Tukey's post-hoc tests was performed. Scale bar in **B-G**= 500 µm, **B'-E'**= 200 µm, H= 200 µm and 50 µm (insets), **I**= 100 µm

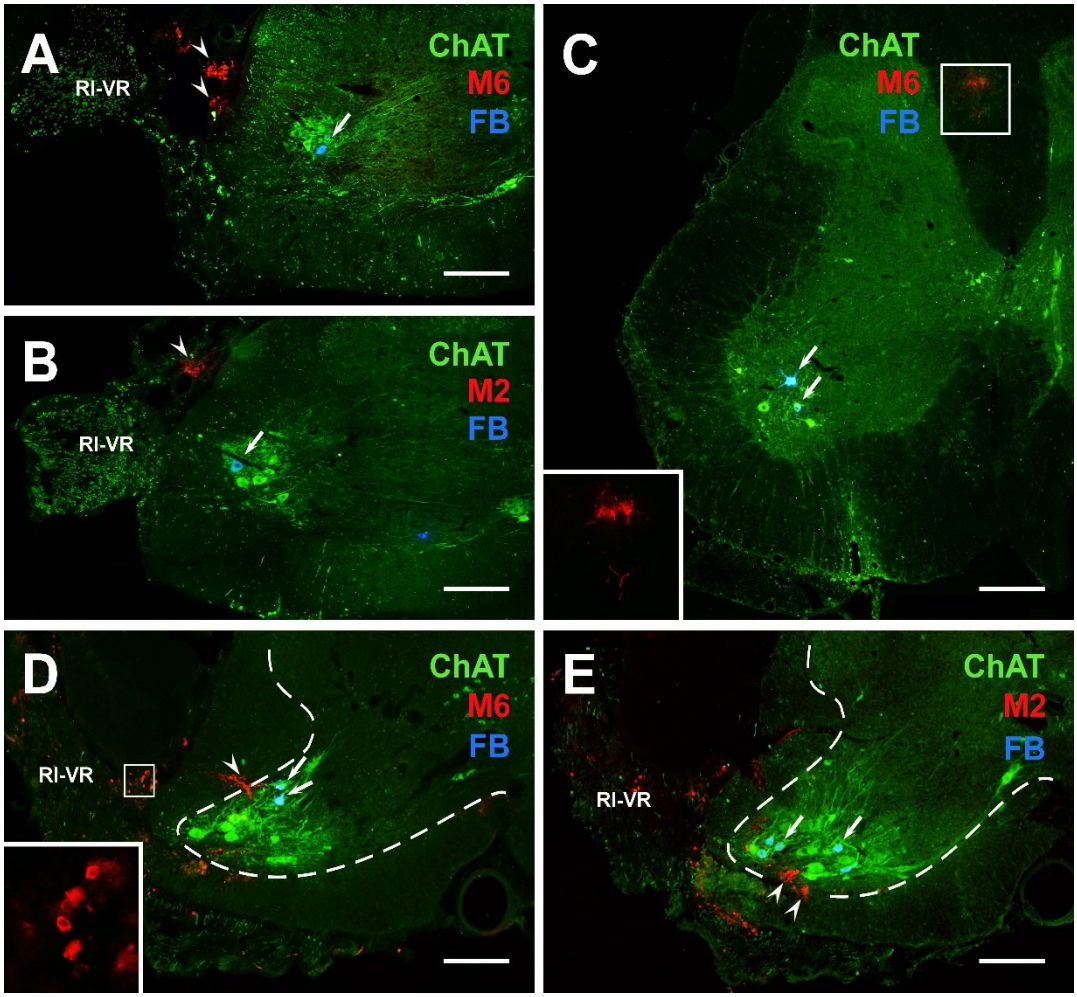

Figure 7. Localization of the derivatives of the grafted stem cells in various experimental paradigms

A and **B** show sections of the spinal cord (ARG-PR group, periradicular grafting) taken at the level where the reimplanted root (RI-VR) is closely apposed to the cord. The few retrogradely labelled motoneurons (arrows, Fast Blue +, FB) colocalise with the numerous surviving ChAT + motoneurons

(green) in the ventral horn. Few surviving undifferentiated cells (arrowheads, M6 + neurons in **A** and M2 + astrocytes in **B**) settled in the dorsal angle between the reimplated L4 root and the dorsolateral surface of the cord. **C** shows surviving (ChAT + , green) and reinnervating (Fast Blue+) motoneurons (arrows) in the ventral horn and stem cell-derived -like cells in the dorsal funiculus of an animal that received intraspinal stem cell graft (ARG group). Inset provides high magnification view of the M6 + cells. **D** and **E** display sections taken from intraradicularly grafted animals (ARG-IR group). Note the greater numbers of retrogradely labelled motoneurons (arrows) within the pool of surviving motoneuron pool (ChAT+, green), Stem cell-derived rounded astrocytes and neurons are present in the reimplanted ventral root (RI-VR, see inset for higher magnification in **D**), however, many of these cells migrated into the affected ventral horn and took up a more differentiated morphological phenotype (arrowheads, M6 + and M2 + cells shown in **D** and **E**, respectively). Scale bar = 200 µm.

Stem cell grafts dramatically improve the reinnervation of hindlimb muscles by the rescued motoneurons

To find out the most effective dose of stem cells we have set experiments where we transplanted increasing numbers of stem cells ($5x10^4$, 1x, 2x and $3x10^5$ stem cells, n=5 in each group) to determine whether motoneuron survival and reinnervation of reimplanted ventral root depend on the number of the grafted cells.

Retrograde labelling from the ventral ramus of the L4 spinal nerve 3 months after grafting revealed that large numbers of axons of surviving motoneurons (up to 65% of the total L4 motoneuron pool) were able to enter the reimplanted root and reinnervate muscles in animals that received a stem cell graft ($3x10^5$ stem cells) at the time of avulsion and reimplantation (ARG animals, Figs. 8A-B). In the non-grafted control animals (AR animals, n=5), however, only minimal numbers of motoneurons (46±5, 4% of the total intact L4 pool) contributed to the reinnervation of the hindlimb muscles (Fig. 8A). Increasing numbers of grafted stem cells ($5x10^4$, 1x, 2x and $3x10^5$ stem cells, n=5 in each group) proved to induce proportionally increasing numbers of surviving motoneurons that reinnervated the targets, suggesting a motoneuron-rescuing mechanism dependent on the amount of factors secreted by the grafted cells (Figs. 8A-B). However, the number of grafted cells that could be utilized to rescue the motoneurons and promote their regeneration exhibited an optimum. Grafts involving more than $3x10^5$ stem cells (e.g. $5x10^5$ or $1x10^6$ stem cells) caused damage to the host cord, thereby

compromising the regenerative effects of the grafted stem cells. Such grafts were therefore excluded from the present study. In the subsequent work reported here each ARG animal received $3x10^5$ stem cells. Morphological reinnervation was confirmed by examinations proving functional reinnervation. The higher numbers of motor units found in the grafted animals (21±1 [ARG] *vs* 4±1 [AR] motor units for the tibialis anterior, and 14±1 [ARG] *vs* 4.5±1 [AR] for the extensor digitorum longus; Figs. 8C-D) produced significantly greater forces in the tibialis anterior (79%±3 operated/intact side [ARG] *vs* 7.5%±2.5 [AR]) and the extensor digitorum longus (73%±3 [ARG] *vs* 13%±4 [AR]) muscles (n=4, Figs. 8E-F).

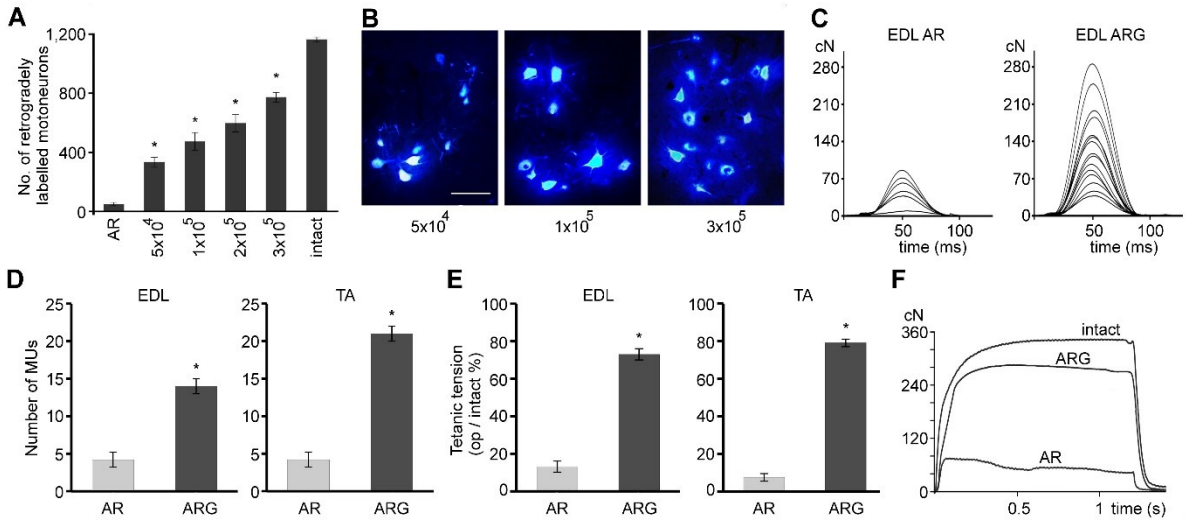

Figure 8. Reinnervation of peripheral targets by injured motoneurons rescued by grafted stem cells

A,B. The extent of reinnervation of peripheral targets depends on the number of grafted stem cells. In control animals (AR), only 46±5 retrogradely labelled cells were found, while the transplantion of $3x10^5$ stem cells resulted in 736±32 reinnervating motoneurons, n=5. **C,D.** The extensor digitorum longus (EDL) and the tibialis anterior (TA) muscles of grafted (ARG) rats are innervated by significantly greater numbers of motor axons than are the muscles of AR animals; individual twitch contractions of motor units (MU) are shown in **C,** n=4. **E,F.** Greater numbers of reinnervating motor axons produced greater maximum tetanic muscle contractions in ARG animals, n=4; individual tetanic curves are shown in **F.** Data are presented as mean +/- S.E.M, $p<0.05$. Data were analysed by applying the non-parametric Mann-Whitney U test or one-way ANOVA analysis with Tukey's post-hoc tests was used. Scale bar in **B**= 100 µm.

Stem cell graft downregulates glial microenvironment in the host cord

We next investigated the glial environment of the injured motoneurons in the ventral horn of grafted (ARG) and control animals (AR). Both astroglial and microglial activity are known to moderate cascades of negative effects on damaged neurons of the spinal cord, although the nature of the microglia/macrophages that participate in certain pathological processes is still controversial (Biber *et al*., 2007; Gaudet *et al.*, 2011). We therefore looked at the glial reactions within the spinal cords of AR and ARG animals in the critical first 10 days after the avulsion injury. At 5 and 10 days after grafting, neuroectodermal stem cell transplantation led to significant decrease in the microglia/macrophage and astroglial reactions throughout segment L4 of ARG animals relative to AR animals (Fig. 9).

Determination of secreted factors expressed in the grafted cord

These data suggested that, in view of the lack of physical contact between the injured and the grafted cells, a paracrine secretory mechanism must be exerted by the graft to decrease the activity of the glial cells of the cord and prevent motoneuron death. To determine the factors acting in the grafted cords, we performed a series of semiquantitative PCR analyses of the segment L4 in ARG and AR animals, concerning neurotrophic and immune factors known to play roles in spinal cord injuries and their experimental treatment (Bartholdi and Schwab, 1997; Ousman and David, 2001). It emerged that on postoperative days 2, 5, 10 and 14 there was no difference between the AR and ARG animals (n=4 in each group) in the mRNA levels of the investigated neurotrophic factors (BDNF and GDNF), but the mRNA levels of the interleukins IL-1-alpha, IL-6 and IL-10, TNF-alpha and MIP-1-alpha were significantly higher in the ARG than in the AR animals, typically at 5 and 10 days following grafting. However, the mRNA production of these factors had declined by 14 days after grafting (Fig. 10).

Differential mRNA expression of cytokines in the stem cells graft and in the ventral horns

To distinguish between graft and host immune factor production, we used the laser microdissection technique to perform a qPCR analysis on identical parts of spinal cord sections (ventral horns) taken from AR and ARG animals and from the stem cell graft (n=5 in each group) The stem cell grafts and the ventral horns of the ARG animals produced

considerable amounts of the cytokines investigated, with appreciable increases by 10 days as compared with 5 days after grafting (Figs. 11A-E); IL-10 proved to be an exception, as it was produced in greater amounts by the grafted cells 5 days after grafting. In contrast, the ventral horns of the AR animals produced increased amounts of the mRNAs of these factors at 5 days, with a moderate decline by 10 days after the avulsion injury; IL-10 was again an exception: it was not produced in the control cords at all (Fig. 11C). The cultured NE-GFP-4C cells (native graft source) did not display detectable levels of the mRNAs of any of the factors. At a survival time of 10 days, the ventral horns of the ARG animals exhibited increased mRNA levels of all the factors, including IL-10, relative to the mRNA levels of the AR animals, suggesting a graft-induced upregulation of these factors at the mRNA level in the host cord.

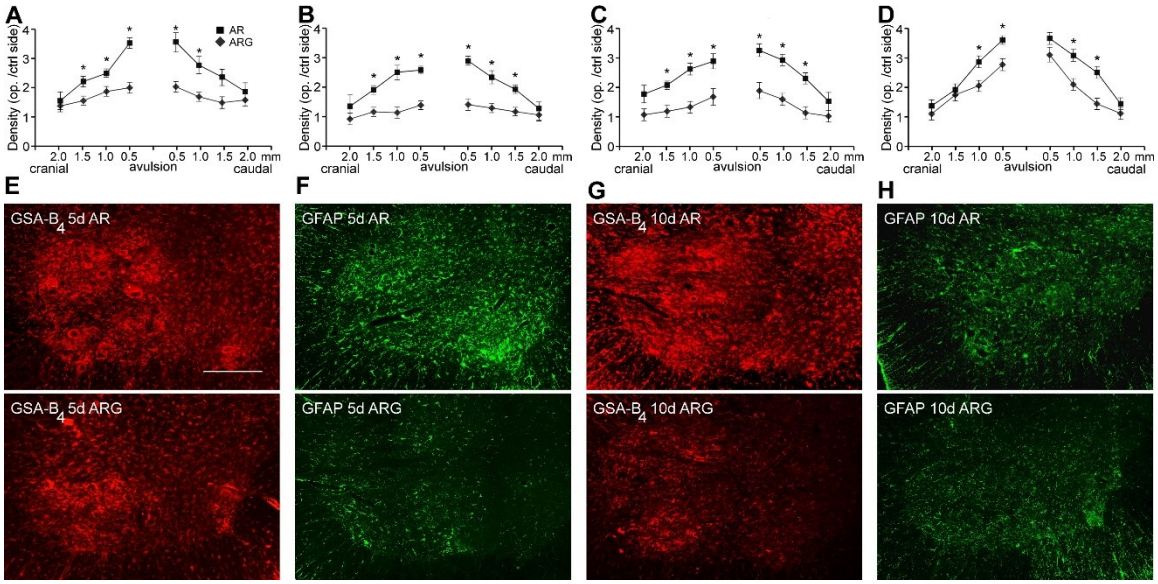

Figure 9. Astrocytic and microglial/macrophage reactions in grafted and control spinal cords

A-H. Reduced astroglial (GFAP) and microglial (GSA B_4 isolectin) densities are shown in spinal segment L4 of ARG animals. Asterisks indicate the significant differences in density between AR and ARG animals at various distances from the site of avulsion, n=5. Data are presented as mean +/- S.E.M, $p<0.05$. The two-way ANOVA analysis with Tukey's post-hoc tests was used. Scale bar in **E**= 250 µm.

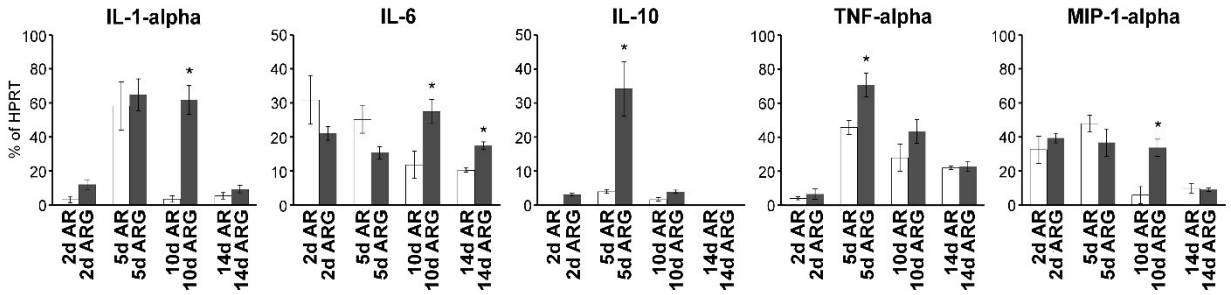

Figure 10. Results of semiquantitative PCR studies on the production of cytokines

Semiquantitative PCR analysis of cytokine mRNA levels in the injured (AR) or grafted (ARG) L4 segment. Only those factors are shown that displayed a significant difference at any timepoint. Note the great amount of IL-10 mRNA produced in the grafted L4 segment of the ARG animals (n=4 in each group). *=significant difference between the ARG and AR animals at the same timepoint. The non-parametric Mann-Whitney U test was used.

Protein expression patterns of cytokines in the grafted cells and in the spinal cord

To test whether the mRNA levels are translated into protein production, the protein expression patterns of these cytokines were studied by immunohistochemistry. Through the use of mouse-specific antibodies, strong immunoreactivity to all five factors was found to be exerted by the grafted cells at 5 days after grafting (Figs. 11F-J). It was noteworthy that the majority, but not all of the grafted cells were immunopositive for the cytokines tested. However, at 10 days postoperatively only the strong expression patterns of IL-6, TNF-alpha and MIP-1-alpha were maintained (Fig. 12B, D and E). The immunofluorescence of IL-1-alpha and IL-10 was confined to some of the stem cells located at the periphery of the graft (Fig. 12A and C). On the other hand, immunohistochemistry with anti-rat/mouse specific antibodies indicated that the ventral horn neurons and glial cells of the ARG animals appeared to produce only IL-6, IL-10 and MIP-1-alpha. The expression patterns were uniform at both 5 and 10 days after grafting. Confocal microscopic analysis of double-labelled sections revealed that the glial IL-6, IL-10 and MIP-1-alpha reactivity was confined to the astrocytes, and not to the microglia/macrophages of the host cord, even though the degree of astrogliosis in the ARG animals was limited (Fig. 13). A similar distribution pattern of these cytokines was observed in the AR animals, but the astroglial density was increased. Despite the relatively high mRNA levels of IL-1-alpha and TNF-alpha, no immunoreactivity to these factors could be detected as compared with the biological positive controls (see Experimental Procedures).

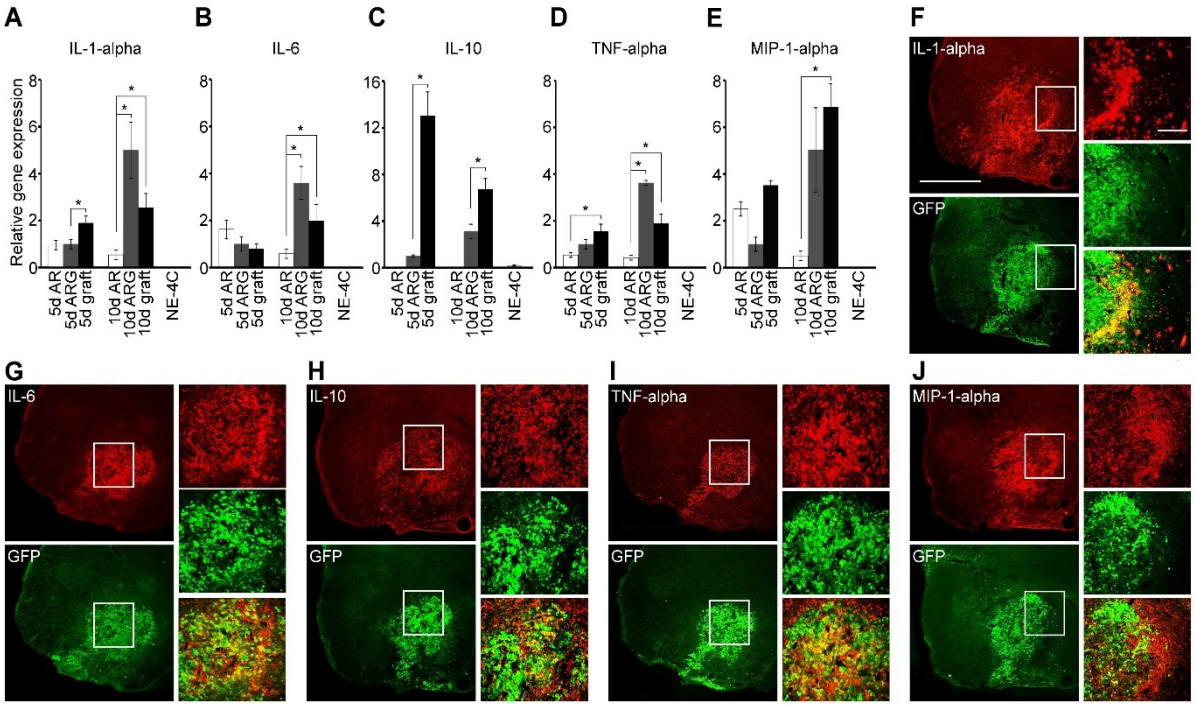

Figure 11. Elevated mRNA levels and immunohistochemical detection of cytokines produced by the grafted stem cells

A-E. Relative gene expression levels of various cytokines in the ventral horns of AR and ARG animals and in the grafts removed by laser microdissection. There were significant increases in the RNA levels of all factors, and of IL-10 in the ventral horns and in the grafts of ARG animals by 10 days after grafting relative to the data at 5 days, n=4. IL-10 was produced only in the grafted cords, mainly by the grafted cells at 5 days after transplantation. Ventral horns of 5d ARG animals are taken as 1 unit. RNA levels of intact ventral horns are not shown as they were negligible. **F-J.** Immunohistochemical detection of the murine factors produced by the grafted cells at 5 days after transplantation. Note the partial expression pattern shown by the grafted cells, especially in the case of MIP-1-alpha, partially due to declining GFP activity. Data are presented as mean +/- S.E.M, $p<0.05$. The one-way ANOVA analysis with Tukey's post-hoc test was used. Scale bar in **F**= 500 μm and 50 μm in insets.

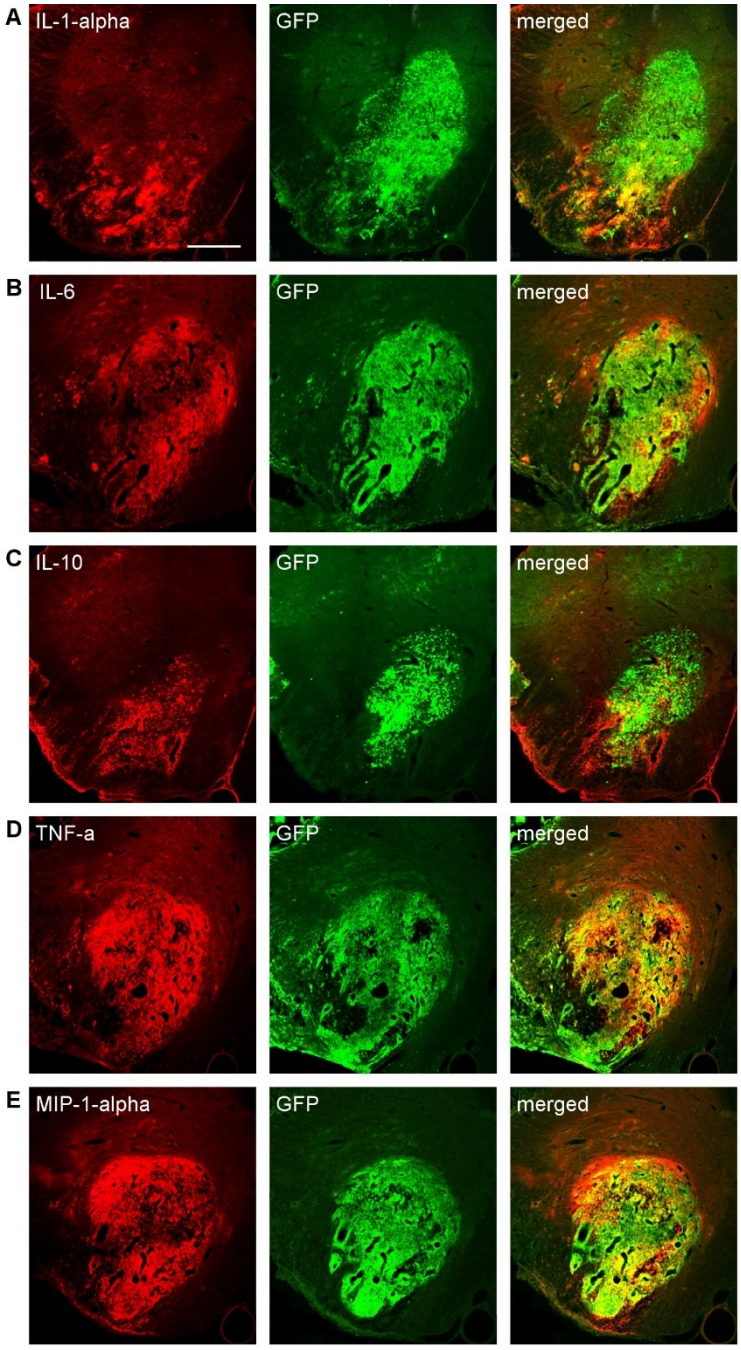

Figure 12. Expression of various cytokines by the grafted stem cells in ARG animals 10 days after surgery

Immunofluorescence images of stem cell grafts in the ventral horns of ARG animals 10 days following grafting. While the immunohistochemistry to IL-6, TNF-alpha and MIP-1-alpha still reveals a strong expression pattern, IL-1-alpha and IL-10 protein expression is limited to a small ventral and peripheral area of the graft. All immunohistochemical analyses were performed with mouse-specific antibodies against cytokines. Scale bar in **A-E**= 200 μm.

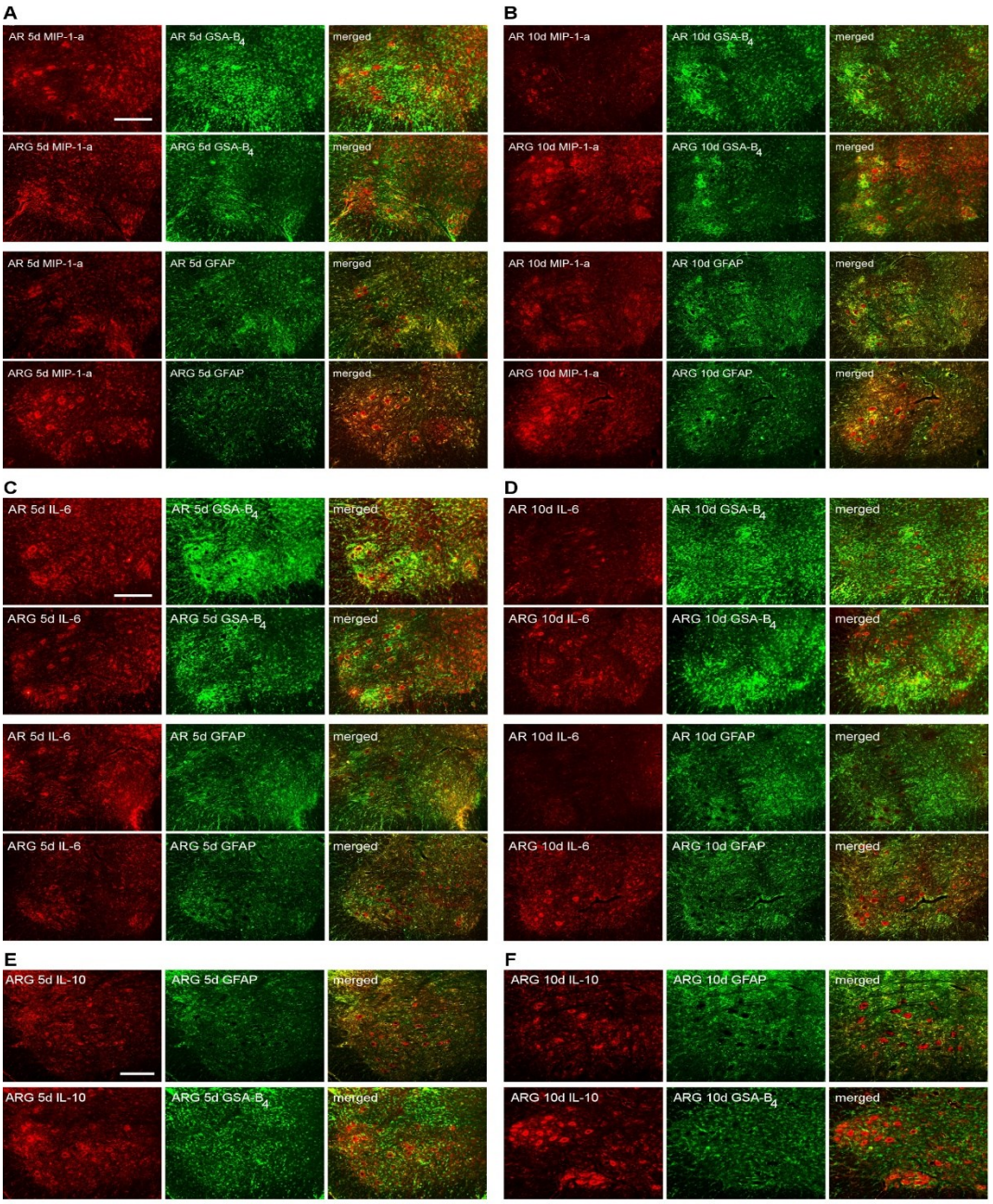

Figure 13. Confocal microscopic analysis of MIP-1-alpha, IL-6 and IL-10 expressions in the host cord

Co-expression of MIP-1-alpha (**A-B**), IL-6 (**C-D**) and IL-10 (**E-F**) and microglial or astrocytic markers (GSA-B_4 isolectin or GFAP, respectively), detected at 5 and 10 days postoperatively in AR and ARG animals. The cytokine expressions are localized to astrocytes and neurons in the ventral horn. Microglial cells do not express the cytokines. No IL-10 immunoreactivity was detected in AR animals (not shown). Scale bar for the MIP-1-alpha and IL-6 panels = 250 μm, for the IL-10 panel = 200 μm.

Function-blocking antibodies abolish the neuroprotective effects of the grafted stem cells

To test whether these cytokines are indeed responsible for inducing the prevention of motoneuron death, for 2 weeks we used osmotic pumps to infuse the mixture of function-blocking mouse-specific antibodies produced against all five factors to the grafts (n=5, ARG + 5-factor neutralization). Indeed, retrograde labelling from the ventral ramus of the L4 spinal nerve revealed virtually as few reinnervating motoneurons after 3 months as in the AR animals (57±5 [ARG+5-factor neutralization], 46±5 [AR]; Figs. 14A,D, and E). However, the question remained as to whether the considerable amount of IL-10 (the only cytokine with anti-inflammatory effects in the peripheral immune system) produced by the grafted cells would alone be able to prevent motoneuron death. In a search for an answer to this question, we set up another function-blocking experiment (n=5, ARG + IL-10 neutralization) in which only the anti-IL-10 mouse-specific function-blocking antibody was infused by osmotic pump to the grafted cord. When the IL-10 function was blocked in this way, the reinnervation was dramatically improved in comparison with that in the AR and ARG + 5-factor neutralization animals (195±10 reinnervating motoneurons, Fig. 14E). In order to test whether the application of an osmotic pump induces a damage in the rescued motoneuron pool, pumps filled with isotype-specific IgG were used and no significant difference relative to the ARG animals was found (n=5, ARG+IgG; 695±44, Fig. 14E). The significant difference in reinnervating motoneuron numbers between the two neutralization groups reveals a strong modulatory role for the other four factors in the injured cord (Fig. 14E and F); the blocking of IL-10 produced by the grafted cells was only partially able to inhibit the beneficial effect of the graft. To establish whether the major beneficial effect of IL-10 involves the survival and/or the reinnervating capacity of the motoneurons, we made use of anti-choline acetyltransferase (ChAT) immunofluorescence to detect and count the surviving and intact motoneurons, including those “silent motoneurons” that are not able to regenerate their axons into the vacated endoneural sheaths of the reimplanted L4 root. The proportion of surviving motoneurons compared to the total $ChAT^+$ motoneuron pool in segment L4 was dramatically increased in the ARG animals but not in the other experimental groups (Fig. 14G), indicating that IL-10 is mainly responsible for the survival of the motoneurons in this experimental paradigm. On the other hand, the proportion of surviving motoneurons that are able to reinnervate peripheral targets (Fig. 14G) was again improved after blockade of the IL-10

function, which suggests an important, but not overwhelming role for IL-10.

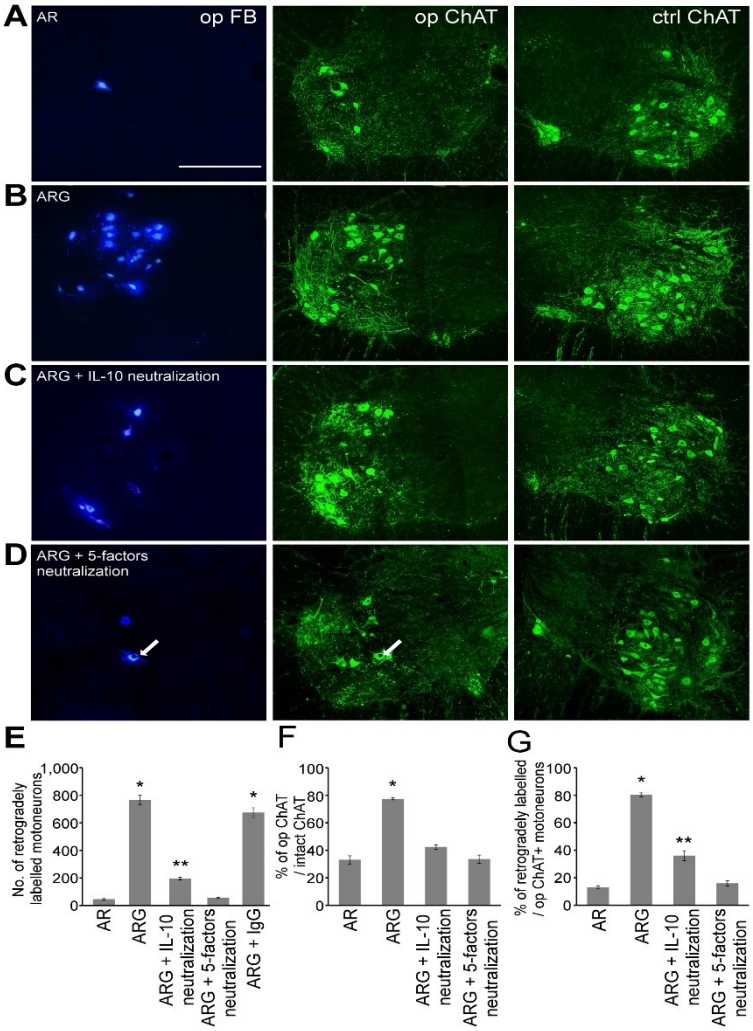

Figure 14. Function-blocking antibodies inhibit the effects of stem cell grafts on motoneuron survival and regeneration

A. Retrogradely labelled (FB^+) and surviving ($ChAT^+$) motoneurons in AR animals. Note the very few reinnervating motoneurons. **B.** Results of retrograde labelling in ARG animals ($3x10^5$ stem cells). Nearly all surviving ($ChAT^+$) cells seem to be able to reinnervate the ventral root. **C,D.** Limited numbers of reinnervating cells can be seen in ARG animals treated with function-blocking antibodies, especially in the case of neutralization against all 5 factors. **E.** Diagram showing the numbers of

retrogradely labelled neurons in various experimental paradigms. Neutralization treatment against all 5 factors resulted in as low numbers of retrogradely labelled neurons as in AR animals, while treatment with isotype-specific IgGs (ARG+IgG) did not yield significantly less motoneuron survival compared with ARG animals, n=5. **F.** The percentage of surviving injured motoneurons is shown by the proportion of $ChAT^+$ operated/intact motoneurons in animals with various experimental paradigms. As neutralization of IL-10 considerably reduces the number of surviving motoneurons, IL-10 appears to be a strong survival factor for injured motoneurons, n=5. **G.** Percentages of reinnervating (FB^+) motoneurons in various groups (FB^+/op. $ChAT^+$ motoneurons). Note the reinnervating ability of motoneurons in ARG animals and the moderate ability after neutralization with IL-10 antibody, n=5. *=significant difference between ARG and AR, ARG+IL-10 neutralization and ARG+5-factor neutralization groups (SEM, $p<0.05$). **=significant difference between ARG+IL-10 neutralization and ARG+5-factor neutralization groups (S.E.M, $p<0.05$). The one-way ANOVA analysis with Tukey's post-hoc test was performed. Scale bar in **A-D**= 250 µm. Data are presented as mean +/- S.E.M.

Discussion

Alternative route providing morphological and functional restitution of hindlimb locomotion by regenerating spinal motoneurons

In this study we have provided evidence, that grafted embryonic neuroectodermal stem cells are able to rescue the vast majority of damaged motoneurons otherwise destined to die. However, rescue of injured motoneurons by grafted stem cells was only successful if the stem cells were placed into the affected segment of the spinal cord or into the reimplanted ventral root of animals whose L4 ventral root was avulsed to bring about motoneuron death.

Adult motoneurons survive if their axons are damaged far from the cell body, but most of them die if the axonal injury is inflicted close to their soma. This latter type of injury is manifested in case of human brachial plexus injuries, where one or more ventral roots suffer traumatic avulsion due to harsh physical forces (Carlstedt 2008). Ventral root avulsion injuries can successfully be modelled in experimental animals and several experimental approaches have been reported to rescue motoneurons with avulsed axons. These experimental strategies are of outstanding importance as the axons of the rescued motoneurons can be redirected to their peripheral targets and this way improved reinnervation of denervated muscles can be achieved (Carlstedt and Cullheim 2000; Carlstedt 2008).

Earlier studies have shown that stem or progenitor cells grafted into the spinal cord following avulsion and reimplantation of one or more spinal ventral roots are able to rescue damaged motoneurons (Hell *et al.*, 2009; Su *et al.*, 2009). Furthermore, it has also been shown that embryonic spinal cord grafts containing neural progenitors induce the survival of the injured motoneurons and also promote the growth of the regenerating motor axons into the reimplanted ventral root and then further along the peripheral nerves until motor fibres reach the skeletal muscles and produce functional reinnervation (Nógrádi and Szabó 2008; Nógrádi *et al.*, 2011).

Grafting NE-GFP-4C stem cells into the spinal cord or into the reimplanted ventral root resulted in equally good survival of injured motoneurons and functional reinnervation. It appears feasible that stem cells placed into the spinal cord are able to rescue motoneurons as they are very closely related to the injured motor pool of the affected segment and the paracrine mechanisms exerted by the graft have a direct effect on the damaged cord. On the

other hand, stem cells transplanted in the reimplanted ventral root are not in the direct vicinity of the motor pool. It can be argued, however, that the amount of molecules secreted by the grafted stem cells was able to reach the intraspinal axon segment and the cell body of the injured motoneurons. The immunhistochemical analysis of the location and differentiation of the intraradicularly grafted cells showed that large numbers of stem cells were present 5 and 10 days after the injury in the reimplanted root, closely related to the spinal cord and regrowing axons that were already present in the root as 10 days after avulsion. It could be noted that the distance between the intraspinal grafts and the rostralmost part of the rescued L4 motoneuron pool is in fact not greater than that of an intraradicular graft and the rostral L4 motoneurons. It is thought that the diffusible factors produced by the grafts may reach the furthermost parts of the L4 segment, no matter whether they are secreted by an intraspinal or by an intraradicular graft. It has been reported that motoneurons after avulsion injury are responding to rescuing strategies if the treatment starts within 10 days following avulsion (Nógrádi *et al.*, 2007). Therefore it appears likely that appropriate numbers of stem cells located in the reimplanted ventral root were able to exert a motoneuron-rescuing effect similar to that found in the case of intraspinally grafted stem cells. Moreover, the stem cells did not migrate into the spinal cord within the first 10 days after grafting, thus their effect was exerted from their original location. It was a surprising finding, that stem cells grafted periradicularly (i.e. around the reimplanted root in a fibrin clot) induced as little reinnervation as spontaneously regenerating surviving L4 motoneurons in the control animals that did not receive stem cells. The immunhistochemical analysis of the location of periradicularly placed stem cells showed that the stem cells and their derivatives were always in the close vicinity of the ventral root and the L4 spinal segment but likely not close enough to the injured motor pool, therefore they could not exert a direct effect on the damaged motoneurons. This view is further strengthened by results of the mapping of the stem cell-derived astrocytes and neurons in the treated spinal cords 3 months after grafting. While few hundreds of stem cell-derived glia- and neuron-like cells were found in the L4 segment of animals that received intraspinal and intraradicular stem cell grafts, no such cells could be located in animals treated with periradicular grafts. These findings suggest that the NE-GFP-4C cells were not able to migrate into the spinal cord from a periradicular location and as a consequence they were not close enough to the injured spinal motoneurons in the critical period of the first 10 days after

avulsion.

Transplantation of stem or neural progenitor cells (Hell *et al.* 2009, Su *et al.* 2009) producing neurotrophic factors or viral-based overexpression of BDNF or GDNF in the spinal cord or in the reimplanted ventral root (Blits *et al.*, 2004, Eggers *et al.*, 2008) induced prominent survival of damaged motoneurons with avulsed axons, but these rescued motoneurons were unable to send their axons into the reimplanted roots due to the enormous sprouting of regenerating axons. On the other hand, our recent experiments have shown that spatiotemporaly limited expression of these neurotrophic factors may induce a limited but still successful regeneration of motoneurons (Pajenda *et al.*, 2014).

Activation of astroglia and microglia following ventral root avulsion-reimplantation

In our study we have shown that intraspinal neuroectodermal stem cell transplantation significantly decreased astroglia and microglia reaction within the affected L4 segment of ARG animals rostral and caudal from the injury site at 5 and 10 days after grafting compared with controls.

It is known that astrocytes have a complex role after CNS injury. In the mature intact CNS they modulate the levels of the excitatory neurotransmitter glutamate, buffer excess potassium in the extracellular space, and regulate neuronal calcium levels (Anderson and Swanson 2000; Norenberg, 1979; Schousboe *et al.*, 2004; rewieved in Walz 2000; Walz *et al.*, 1984, Parpura *et al.*, 1994).

Astrocytes that are located at the site of injury become reactive and contribute to the glia scar that inhibits axon regeneration. However, they produce various factors that protect neurons and express various chemokines that can attract macrophages from the periphery to the site of injury (Strack *et al.*, 2002).

We found, that host astrocytes in the grafted cord produced IL-6, IL-10 and MIP-1-alpha. Expression of these three cytokines were uniform at postoperative days 5 and 10 after grafting even though the extent of astrogliosis was limited in grafted animals. A similar distribution pattern of these cytokines was observed in the control animals, whereas the astroglial density was increased. Although we assume that despite the similar protein expression pattern in the two groups the decreased astrocyte reaction in grafted animals may provide better environment to the motoneuron survival.

Following CNS injury microglia activation is characterized by a number of biochemical and functional changes (Cullheim and Thams, 2007). Thus, activated microglia can produce *N*-methyl-d-aspartate (NMDA) receptor agonists, free oxygen radicals, nitric oxide, proteases and cytokines (Giulian *et al.*, 1993; Chao *et al.*, 1992; Moore and Thanos, 1996). In the first 10 days following avulsion injury limited microglia reaction could be detected in the L4 segment in intraspinally grafted animals compared with controls. This observation suggests that a limited microglia reaction provides a better milieu for motoneuron survival.

Immunomodulatory molecules produced by grafted neuroectodermal stem cells prevented motoneuron death following ventral root avulsion

In this study the pro- and anti-inflammatory cytokines have been shown to prevent motoneuron death after ventral root avulsion.

Recent findings form our and other laboratories suggest that the rescue of injured neurons within the CNS by a composition of anti- and pro-inflammatory cytokines may be due to a twofold mechanism: First, the glial reactions and glutamate toxicity in the host environment are significantly reduced, second, at least some of the cytokines, especially IL-10 are thought to exert a direct neuroprotective effect on the injured neurons themselves.

Numerous studies have provided evidence that the anti-inflammatory cytokine, IL-10, would suppress mechanisms leading to cell death and decrease astroglia and microglia reactions (Bachis *et al.*, 2001, Boyd *et al.*, 2003). Administration of IL-10 after traumatic or excitotoxic spinal cord injury promoted the survival of injured neurons, improved recovery of motor function and reduced tissue damage (Bethea *et al.*, 1999; Jackson *et al.*, 2005). On the other hand, in an other study in vivo application of IL-10 did not enhance axon growth and motor recovery (Takami *et al.*, 2002). Recently the anti-inflammatory cytokine IL-10 has been shown to induce a number of signaling cascades through IL-10 receptor leading to the activation of the p50/p65 NfκB-mediated antiapoptotic pathway in neurons (Zhou *et al.*, 2009a, 2099b). As an end result, increased levels of Bcl-2 and Bcl-xL and reduced cytochrome-C release and caspase activation were found and these changes are thought to contribute to the survival of injured motoneurons.

Proinflammatory cytokines such as IL-1-alpha, IL-6, TNF-alpha rapidly produced in spinal cord. These cytokines have overlapping function in the CNS. Recent studies have provided

controversial date on the effect of these cytokines. They reportedly modulate glutamaterg transmission, synaptic plasticity or NMDA activation and contribute to the survival of injured neurons (Coogan *et al.*, 1997; Li *et al.*, 1997). Activation of NfκB, JAK-STAT and/or PI3K-Akt pathways activate various signal transduction pathways in the cells resulting in protection against metabolic-excitotoxic insults, stabilize [Ca2+] homeostasis and increased expression of the calcium-binding protein calbindin. (Wang *et al.*, 2009; Cheng *et al.*, 1994)

Mechanical injury and neuroinflammatory processes induce chemokine actions via the upregulated chemokine receptors. MIP-1-alpha can act via G-protein–coupled receptors and the control of cytokine profiles in the injured CNS (Rossi and Zlotnik, 2000; Mennicken *et al.*, 1999*)*. However the exact role of MIP-1-alpha in neuroprotective mechanisms remains to be elucidated in future studies.

Functional blocking of IL-10 in our experiment has shown that blocking of IL-10 secreted by grafted cells resulted in similar motoneuron survival as in control group or 5-factor blocking group. Although the number of surviving motoneurons in the IL-10 blocking group showed the same results as a control group but number of reinnervating motoneurons was signficantly greater than in 5-factor blocking group. These data suggested that IL-1-alpha, IL-6, TNF-alpha and MIP-1-alpha have a major role in promoting regeneration than in inducing survival of injured motoneurons.

These data strongly support the view that acute or sub-acute exposure of the highly vulnerable injured motoneuron pool to these pro-inflammatory cytokines is not deleterious, although longer expression patterns of these cytokines is already thought to induce toxic effects. The fact, that the grafted stem cells remain clustered at the site of grafting for 10 days and show only limited differentiation along with significant rates of cytokine expression levels suggest, that this short period of time of stem cell differentiation provides satisfactory neuroprotection for the injured motoneurons along with considerable depression of macrophage and astrocyte activation. It is noteworthy that the stem cell grafts induced expression of some of the cytokines, including IL-10 in the host ventral horn, and this was likely to contribute to their neuroprotective effects. The rapid differentiation process and migration of stem cells appears to cease cytokine expression after this beneficial period of time.

These data, in conjunction with our findings, strongly suggest that pro-inflammatory and anti-inflammatory cytokines selectively secreted by grafted stem cells act in concert to save

motoneurons and to promote reinnervation of the target muscles. These results raise the opportunity to investigate whether local treatment of injured motoneurons with a well-defined set and dose of cytokines may bring about the similarly great extent of cell rescue and reinnervation as treatment with stem cells.

Conclusions

In conclusion, it can be stated that stem cells that are able to rescue the vast majority of injured motoneurons destined to die following transplantation into the injured spinal cord segment are also able to induce the same effect if they are grafted into the reimplanted ventral root, close to the axons of the injured motor pool. These results suggest that the diffusible factors that modulate the environment of injured motoneurons are able to reach the ventral horn from more remote positions provided they are located still within the boundaries of the spinal cord and related spinal roots.

Furthermore, cytokines produced by grafted neuroectodermal stem cells are likely to rescue damaged motoneurons following ventral root avulsion injury via two distinct mechanisms. Moreover, grafted stem cells interact with the host environment and induce a pattern of cytokine expression by host neurons and astrocytes. It is suggested that the anti- and pro-inflammatory cytokines have a strong modulatory function in the CNS that promote the prevention of neuronal cell death and induce regeneration.

Acknowledgements

I am indebted to Prof. Antal Nógrádi (Head of Laboratory of Neural Regeneration at the Department of Anatomy, Histology and Embryology, Faculty of Medicine, University of Szeged) for his professional mentorship and scientific guidance for my research.

I would like to express my gratitude to Gábor Márton for his professional help in figures design and consultive support.

Special thanks to all member Laboratory of Neural Regeneration, namely Ferencné Katona, Attiláné Kovács,, Tamás Bellák, Zoltán Fekécs, László Gál and Dr. Péter Balázs Kocsis.

I would like to express my thanks to my co-author Dr. Gholam Pajenda (Department for Trauma Surgery, Medical University Vienna, Vienna, Austria) who helped with the surgical procedure in Ludwig Boltzmann Institute for Experimental and Clinical Traumatology, Vienna, Austria.

My thanks are due to my co-author colleagues, Georg Feichtinger, and Professor Heinz Redl for their professional help in the semiquantitatve PCR analysis that was performed in Ludwig Boltzmann Institute for Experimental and Clinical Traumatology, Vienna, Austria.

The laser microdissection and qPCR measurements were performed in VetCORE Technology Centre for Research at the University of Veterinary Medicine in Vienna, Austria. I am indebted to Sonja Sabitzer and Professor Dieter Klein for their professional help.

Finally, I would like to express my special thanks to my family, and first of all, to my wife, Rita Pajer-Józsa, who supported in the recent period of my life, and helped me through the difficult periods of writing my thesis.

References

Airaksinen MS, Saarma M. The GDNF family: signalling, biological functions and therapeutic value. Nat Rev Neurosci, **2002** 3, 383-394.

Aloisi F, De Simone R, Columba-Cabezas S, Levi G. Opposite effects of interferon-gamma and prostaglandin E2 on tumor necrosis factor and interleukin-10 production in microglia: a regulatory loop controlling microglia pro- and anti-inflammatory activities. J Neurosci Res, **1999** 56, 571–580.

Anderson CM, Swanson RA. Astrocyte glutamate transport: review of properties, regulation, and physiological functions. Glia, **2000** 32, 1-14.

Bachis A, Colangelo AM, Vicini S, Doe PP, De Bernardi MA, Brooker G, Mocchetti I. Interleukin-10 prevents glutamate-mediated cerebellar granule cell death by blocking caspase-3-like activity. J Neurosci, **2001** 21, 3104–3112.

Bartholdi D, Schwab ME. Expression of pro-inflammatory cytokine and chemokine mRNA upon experimental spinal cord injury in mouse: an in situ hybridization study. Eur J Neurosci, **1997** 9, 1422-1438.

Battista D, Ferrari CC, Gage FH, Pitossi FJ. Neurogenic niche modulation by activated microglia: Transforming growth factor beta increases neurogenesis in the adult dentate gyrus. Eur J Neurosci, **2006** 23, 83–93.

Beattie MS, Bresnahan JC, KomonJ, Tovar CA, Van Meter M, Anderson DK. Faden AI, Hsu CY, Noble LJ, Salzman S, Young W. Endogenous repair after spinal cord contusion injuries in the rat. Exp Neurol, **1997** 148, 453-463.

Beattie MS, Ferguson AR, Bresnahan JC. AMPA-receptor trafficking and injury-induced cell death. Eur J Neurosci, **2010** 32, 290-7.

Bergerot A, Shortland PJ, Anand P, Hunt SP, Carlstedt T. Co-treatment with riluzole and GDNF is necessary for functional recovery after ventral root avulsion injury. Exp Neurol, **2004** 187, 359-66

Bessis A, Bechade C, Bernard D, Roumier A. Microglial control of neuronal death and synaptic properties. Glia, **2007** 55, 233–38.

Bethea JR, Nagashima H, Acosta MC, Briceno C, Gomez F, Marcillo AE, Loor K, Green J, Dietrich WD. Systemically administered interleukin-10 reduces tumor necrosis factor-alpha production and significantly improves functional recovery following traumatic spinal cord injury in rats. J Neurotrauma, **1999** 16, 851–863.

Biber K, Neumann H, Inoue K, Boddeke HW. Neuronal 'On' and 'Off' signals control microglia. Trends Neurosci, **2007** 30, 596-602.

Blinzinger K, Kreutzberg G. Displacement of synaptic terminals from regenerating motor neurons by microglial cells. Z Zellforsch Mikrosk Anat, **1968** 85, 145–157.

Blits B, Carlstedt TP, Ruitenberg MJ, de Winter F, Hermens WT, Dijkhuizen PA, Claasens JW, Eggers R, van der Sluis R, Tenenbaum L, Boer GJ, Verhaagen J. Rescue and sprouting of motoneurons following ventral root avulsion and reimplantation combined with intraspinal adeno-associated viral vector-mediated expression of glial cell line-derived neurotrophic factor or brain-derived neurotrophic factor. Exp Neurol, **2004** 189, 303-16.

Bottai D, Cigognini D, Madaschi L, Adami R, Nicora E, Menarini M, Di Giulio AM, Gorio A. Embryonic stem cells promote motor recovery and affect inflammatory cell infiltration in spinal cord injured mice. Exp Neurol, **2010** 223, 452-63.

Boyd, ZS, Kriatchko, A, Yang, J, Agarwal, N, Wax, MB, Patil, RV. Interleukin-10 receptor signaling through STAT-3 regulates the apoptosis of retinal ganglion cells in response to stress. Invest Ophthalmol Vis Sci, **2003** 44, 5206–5211.

Brännström T, Havton L, Kellerth JO. Restorative effects of reinnervation on the size and dendritic arborization patterns of axotomized cat spinal alpha-motoneurons. J Comp Neurol, **1992** 318, 452-61.

Carlson NG, Bacchi A, Rogers SW, Gahring LC. Nicotine blocks TNF-alpha-mediated neuroprotection to NMDA by an alpha-bungarotoxin-sensitive pathway. J Neurobiol, **1998** 35, 29-36.

Carlson NG, Wieggel WA, Chen J, Bacchi A, Rogers SW, Gahring LC. Inflammatory cytokines IL-1 alpha, IL-1 beta, IL-6, and TNF-alpha impart neuroprotection to an excitotoxin through distinct pathways. J Immunol, **1999** 163, 3963-8.

Carlstedt T, Cullheim S. Spinal cord motoneuron maintenance, injury and repair. Prog Brain Res, **2000** 127, 501-14. Review

Carlstedt T. Nerve fibre regeneration across the peripheral-central transitional zone. J Anat **1997** 190, 51-6. Review.

Carlstedt T. Root repair review: basic science background and clinical outcome. Restor Neurol Neurosci, **2008** 26, 225-41. Review

Chao CC, Hu S, Ehrlich L, Peterson PK. Interleukin-1 and tumor necrosis factor-alpha synergistically mediate neurotoxicity: involvement of nitric oxide and of N-methyl-D-aspartate receptors. Brain Behav Immun, **1995** 4, 355-65.

Chao CC, Hu S, Molitor TW, EG Shaskan EG, Peterson PK. Activated microglia mediate neuronal cell injury via a nitric oxide mechanism. J Immunol, **1992** 149, 2736–2741.

Cheng B, Christakos S, Mattson MP. Tumor necrosis factors protect neurons against

metabolic-excitotoxic insults and promote maintenance of calcium homeostasis. Neuron, **1994** 12, 139-53.

Clarke SR, Shetty AK, Bradley JL, Turner, DA. Reactive astrocytes express the embryonic intermediate neurofilament nestin. Neuroreport, **1994** 5, 1885-1888.

Coogan A, O'Connor JJ. Inhibition of NMDA receptor-mediated synaptic transmission in the rat dentate gyrus in vitro by IL-1b. Neuroreport, **1997** 8, 2107-2110.

Corvino V, Businaro R, Geloso MC, Bigini P, Cavallo V, Pompili E. S100B protein and 4-hydroxynonenal in the spinal cord of wobbler mice. Neurochem Res, **2003** 28, 341-345.

Costa S, Planchenault T, Charriere-Bertrand C, Mouche, Y, Fages C, Juliano S. Astroglial permissivity for neuritic outgrowth in neuron-astrocyte cocultures depends on regulation of laminin bioavailability. Glia, **2002** 37, 105-113.

Cullheim S, Fleshman JW, Glenn LL, Burke RE. Membrane area and dendritic structure in type-identified triceps surae alpha motoneurons. J Comp Neurol, **1987a** 255, 68-81.

Cullheim S, Fleshman JW, Glenn LL, Burke RE. Three-dimensional architecture of dendritic trees in type-identified alpha-motoneurons. J Comp Neurol, **1987b** 255, 82-96.

Cullheim S, Kellerth JO. A morphological study of the axons and recurrent axon collaterals of cat sciatic alpha-motoneurons after intracellular staining with horseradish peroxidase. Comp Neurol, **1978** 178, 537-57.

Cullheim S, Thams S. The microglial networks of the brain and their role in neuronal network plasticity after lesion. Brain Research Reviews, **2007** 55, 89–96.

Demeter K, Herberth B, Duda E, Domonkos A, Jaffredo T, Herman JP, Madarász E. Fate of cloned embryonic neuroectodermal cells implanted into the adult, newborn and embryonic forebrain. Exp Neurol, **2004** 188, 254-67.

Eggers R, Hendriks WT, Tannemaat MR, van Heerikhuize JJ, Pool CW, Carlstedt TP, Zaldumbide A, Hoeben RC, Boer GJ, Verhaagen J. Neuroregenerative effects of lentiviral vector-mediated GDNF expression in reimplanted ventral roots. J Mol Cell Neurosci, **2008** 39,105-17.

English AW, Meador W, Carrasco DI. Neurotrophin-4/5 is required for the early growth of regenerating axons in peripheral nerves. Eur J Neurosci, **2005** 21, 2624-2634.

Gaudet AD, Popovich PG, Ramer MS. Wallerian degeneration: gaining perspective on inflammatory events after peripheral nerve injury. J Neuroinflammation, **2011** 8, 1-13.

Giulian D, Vaca K, Corpuz M. Brain glia release factors with opposing actions upon neuronal survival. J Neurosci, **1993** 13, 29–37.

Ha BK, Vicini S, Rogers RC, Bresnahan JC, Burry RW, Beattie MS. Kainate-induced excitotoxicity is dependent upon extracellular potassium concentrations that regulate the activity of AMPA/KA type glutamate receptors. J Neurochem, **2002** 83, 934-45.

Hamers FPT, Koopmans GC Joosten EAJ. Catwalk-assisted gait analysis in the assessment of spinal cord injury. J Neurotrauma, **2006** 23, 537-548.

Hamers FPT, Lankhorst AJ, van Laar TJ, Veldhuis WB Gispen WH. Automated quantitative gait analysis during overground locomotion in the rat: its application to spinal cord contusion and transection injuries. J Neurotrauma, **2001** 18, 187-201.

Hammarberg H, Piehl F, Risling M, Cullheim S. Differential regulation of trophic factor receptor mRNAs in spinal motoneurons after sciatic nerve transection and ventral root avulsion in the rat J Comp Neurol, **2000** 426, 587-601.

Havton L, Kellerth JO. Regeneration by supernumerary axons with synaptic terminals in spinal motoneurons of cats. Nature, **1987** 325, 711-4.

Hell RC, Costa MM, Goes AM, Oliveira AL. Local injection of BDNF producing mesenchymal stem cells increases neuronal survival and synaptic stability following ventral root avulsion. Neurobiol Dis, **2009** 33, 290-300.

Henderson CE, Camu W, Mettling C, Gouin A, Poulsen K,Karihaloo M, Rullamas J, Evans T, McMahon SB, Armanini MP. Neurotrophins promote motor neuron survival and are present in embryonic limb bud. Nature, **1993** 363, 266-270.

Herberth B, Pataki A, Jelitai M, Schlett K, Deák F, Spät A, Madarász E. Changes of KCl sensitivity of proliferating neural progenitors during in vitro neurogenesis. J Neurosci Res, **2002** 67, 574-82.

Hertz L, Drejer J, Schousboe A. Energy metabolism in glutamatergic neurons, GABAergic neurons and astrocytes in primary cultures. Neurochem Res, **1988** 13, 605-610.

Hickey WF, Kimura H. Perivascular microglial cells of the CNS are bone marrow-derived and present antigen in vivo. Science, **1988** 239, 290–2.

Höke A, Redett R, Hameed H, Jari R, Zhou C, Li ZB, Griffin JW, Brushart TM. Schwann cells express motor and sensory phenotypes that regulate axon regeneration. J Neurosci, **2006** 26, 9646-55.

Ikeda O, Murakami M, Ino H, Yamazaki M, Nemoto T, Koda M. Acute up-regulation of brain-derived neurotrophic factor expression resulting from experimentally induced injury in the rat spinal cord. Acta Neuropathol, **2001** 102, 239-245.

Jackson CA, Messinger J, Peduzzi JD, Ansardi DC, Morrow CD. Enhanced functional recovery from spinal cord injury following intrathecal or intramuscular administration of poliovirus replicons encoding IL-10. Virology, **2005** 336, 173–183.

Jankowska E, Lundberg A. Interneurones in the spinal cord. Trends Neurosci, **1981** 4, 230-233

Johnston IP, Sears TA. Ultrastructure of axotomized alpha and gamma motoneurons in the cat thoracic spinal cord. Neuropathol Appl Neurobiol, **1989** 15, 149-63.

Kiefer R, Schweitzer T, Jung S, Toyka KV, Hartung HP. Sequential expression of transforming growth factor-beta1 by T-cells, macrophages, and microglia in rat spinal cord during autoimmune inflammation. J Neuropathol Exp Neurol, **1998** 57, 385–395.

Kigerl KA, Gensel JC, Ankeny DP, Alexander JK, Donnelly DJ, Popovich PG. Identification of two distinct macrophage subsets with divergent effects causing either neurotoxicity or regeneration in the injured mouse spinal cord. J Neurosci, **2009** 29, 13435–44.

Koliatsos VE, Price WL, Pardo CA, Price DL. Ventral root avulsion: an experimental model of death of adult motor neurons. J Comp Neurol, **1994** 342, 35-44.

Környei Z, Szlávik V, Szabó B, Gócza E, Czirók A, Madarász E. Humoral and contact interactions in astroglia/stem cell co-cultures in the course of glia-induced neurogenesis. Glia, **2005** 49, 430-44.

Krenz NR, Weaver LC. Nerve growth factor in glia and inflammatory cells of the injured rat spinal cord. J Neurochem, **2000** 74, 730-739.

Lagerbäck PA, Ronnevi LO, Cullheim S, Kellerth JO. An ultrastructural study of the synaptic contacts of alpha-motoneurone axon collaterals. I. Contacts in lamina IX and with identified alpha-motoneurone dendrites in lamina VII. Brain Res, **1981a** 207, 247-66.

Lagerbäck PA, Ronnevi LO, Cullheim S, Kellerth JO. An ultrastructural study of the synaptic contacts of alpha 1-motoneuron axon collaterals. II. Contacts in lamina VII. Brain Res, **1981b** 222, 29-41.

Lenhossek, v. " Ueber den Bau der Spinalganglienzellen des Menschen." Arch f Psychiat u Nervenkr, XXIX, **1895**.

Li Y, Raisman G. Schwann cells induce sprouting in motor and sensory axons in the adult rat spinal cord. J Neurosci, **1994** 14, 4050-63.

Li AJ, Katafuchi T, Oda S, Hori T, Oomura Y. Interleukin-6 inhibits long-term potentiation in rat hippocampal slices. Brain Res, **1997** 748, 30-38.

Lindå H, Risling M, Cullheim S. Dendraxons' in regenerating motoneurons in the cat: do dendrites generate new axons after central axotomy? Brain Res, **1985** 358, 329-33.

Liu JS, Amaral TD, Brosnan CF, Lee SC. IFNs are critical regulators of IL-1 receptor antagonist and IL-1 expression in human microglia. J Immunol, **1998** 161, 1989–1996.

Liu Z, Qiu YH, Li B, Ma SH, Peng Y. Neuroprotection of interleukin-6 against NMDA-induced apoptosis and its signal-transduction mechanisms. Neurotox Res, **2011** 19, 484-95.

Lowrie MB, Krishnan S, Vrbova G. Permanent changes in muscle and motoneurones induced by nerve injury during a critical period of development of the rat. Brain Res, **1987** 428, 91-101.

Maurer M, von Stebut E. Macrophage inflammatory protein-1. Int J Biochem Cell Biol, **2004** 36, 1882-6.

Mennicken F, Maki R, De Souza EB, Quirion R. Chemokines and chemokine receptors in the CNS: a possible role in neuroinflammation and patterning Trends Pharmacol Sci **1999** 20, 73–78.

Mills CD, Fullwood SD, Hulsebosch CE. Changes in metabotropic glutamate receptor expression following spinal cord injury. Exp Neurol, **2001a** 170, 244-57.

Mills CD, Xu GY, McAdoo DJ, Hulsebosch CE. Involvement of metabotropic glutamate receptors in excitatory amino acid and GABA release following spinal cord injury in rat. J Neurochem, **2001b** 79, 835-48.

Moore S, Thanos S. The concept of microglia in relation to central nervous system disease and regeneration. Prog Neurobiol, **1996** 48, 441–460.

Morgenstern DA, Asher RA, Fawcett JW. Chondroitin sulphate proteoglycans in the CNS injury response. Prog Brain Res, **2002** 137, 313-332.

Nimmerjahn A, Kirchhoff F, Helmchen F. Resting microglial cells are highly dynamic surveillants of brain parenchyma in vivo. Science, **2005** 308, 1314–18.

Nissl F., Ueber die sogenannten Granula der Nervenzellen. Neurol Contr, **1894** 13, 676.

Nógrádi A, Pajer K, Márton G. The role of embryonic motoneuron transplants to restore the lost motor function of the injured spinal cord. Ann Anat, **2011** 193, 362-70.

Nógrádi A, Szabó A, Pintér S, Vrbová G. Delayed riluzole treatment is able to rescue injured rat spinal motoneurons. Neuroscience, **2007** 144, 431-8.

Nógrádi A, Szabó A. Transplantation of embryonic neurones to replace missing spinal motoneurones. Restor Neurol Neurosci, **2008** 26, 215-23. Review

Nógrádi A, Vrbová G. The effect of riluzole treatment in rats on the survival of injured adult and grafted embryonic motoneurons. Eur J Neurosci, **2001** 13, 113-8.

Nogradi A, Vrbova G. Improved motor function of denervated rat hindlimb muscles induced by embryonic spinal cord grafts. Eur J Neurosci, **1996** 8, 2198-203.

Norenberg MD. Distribution of glutamine synthetase in the rat central nervous system. J Histochem Cytochem, **1979** 27, 756-762.

Novikov L, Novikova L, Kellerth JO. Brain-derived neurotrophic factor promotes survival and blocks nitric oxide synthase expression in adult rat spinal motoneurons after ventral root avulsion. Neurosci Lett, **1995** 200, 45-8.

Novikov L, Novikova L, Kellerth JO. Brain-derived neurotrophic factor promotes axonal regeneration and long-term survival of adult rat spinal motoneurons in vivo. Neuroscience, **1997** 79, 765-774.

Ousman SS, David S. MIP-1alpha, MCP-1, GM-CSF, and TNF-alpha control the immune cell response that mediates rapid phagocytosis of myelin from the adult mouse spinal cord. J Neurosci, **2001** 21, 4649-4656.

Pajenda G, Hercher D, Márton G, Pajer K, Feichtinger GA, Maléth J, Redl H, Nógrádi A. Spatiotemporally limited BDNF and GDNF overexpression rescues motoneurons destined to die and induces elongative axon growth. Exp Neurol, **2014** 261, 367-76.

Parpura V, Basarsky TA, Liu F, Jeftinija K, Jeftinija S, Haydon PG. Glutamate-mediated astrocyte-neuron signaling. Nature, **1994** 369, 744-747.

Pintér S, Gloviczki B, Szabó A, Márton G, Nógrádi A. Increased survival and reinnervation of cervical motoneurons by riluzole after avulsion of the C7 ventral root. J Neurotrauma, **2010** 12, 2273-82

Regan RF. The vulnerability of spinal cord neurons to excitotoxic injury: comparison with cortical neurons. Neurosci Lett, **1996** 213, 9-12.

Rexed B. A cytoarchitectonic atlas of the spinal cord in the cat. J Comp Neurol, **1954** 100, 297-379.

Rexed B. The cytoarchitectonic organization of the spinal cord in the cat. J Comp Neurol, **1952** 96, 415-495.

Risling M, Sörbye K, Cullheim S. Aberrant regeneration of motor axons into the pia mater after ventral root neuroma formation. Brain Res. **1992** 570, 27-34.

Romanes GJ. The motor columns of the spinal cord. Prog Brain Res, **1964** 11, 93-116
Rossi D, Zlotnik A. The biology of chemokines and their receptors. Ann Rev Immunol, **2000** 18, 217–242.

Rothstein, J D, Dykes-Hoberg, M, Pardo, C A, Bristol, L A, Jin L, Kuncl, RW. Knockout of glutamate transporters reveals a major role for astroglial transport in excitotoxicity and clearance of glutamate. Neuron, **1996** 16, 675-686.

Rothwell NJ, Luheshi GN. Interleukin 1 in the brain: biology, pathology and therapeutic target. Trends Neurosci, **2000** 12, 618-25.

Sariola H, Saarma MJ. Novel functions and signalling pathways for GDNF. Cell Sci, **2003** 116, 3855-62.

Scheibel ME, Scheibel AB. Terminal axonal patterns in cat spinal cord Ist ed The lateral corticospinal tract. Brain Res, **1966a** 2, 333-350.

Scheibel ME, Scheibel AB. Spinal motoneurons, interneurons and Renshaw cells A Golgi study. Arch Ital Biol, **1966b** 104, 328-353.

Schlett K, Herberth B, Madarász E. In vitro pattern formation during neurogenesis in neuroectodermal progenitor cells immortalized by p53-deficiency. Int J Dev Neurosci, **1997** 15, 795-804.

Schlett K, Madarász E. Retinoic acid induced neural differentiation in a neuroectodermal cell line immortalized by p53 deficiency. J Neurosci Res, **1997** 47, 405-15.

Schomburg ED. Spinal sensorimotor systems and their supraspinal control. Neurosci Res, **1990** 7, 265-340.

Schousboe A, Sarup A, Bak LK, Waagepetersen HS, Larsson OM. Role of astrocytic transport processes in glutamatergic and GABAergic neurotransmission. Neurochem Int, **2004** 45, 521-527.

Strack A, Asensio VC, Campbell IL, Schluter D, Deckert M. Chemokines are differentially expressed by astrocytes, microglia and inflammatory leukocytes in Toxoplasma encephalitis and critically regulated by interferon-gamma. Acta Neuropathol, **2002** 103, 458-468.

Streit WJ, Graeber M, Kreutzberg G. Functional plasticity of microglia: a review. Glia, **1988** 1, 301–307.

Streppel M, Azzolin N, Dohm S, Guntinas-Lichius O, Haas C, Grothe C, Wevers A, Neiss WF, Angelov DN. Focal application of neutralizing antibodies to soluble neurotrophic factors reduces collateral axonal branching after peripheral nerve lesion. Eur J Neurosci, **2002** 15, 1327-1342.

Su H, Yuan Q, Qin D, Yang X, Wong WM, So KF, Wu W. Ventral root re-implantation is better than peripheral nerve transplantation for motoneuron survival and regeneration after spinal root avulsion injury. BMC Surg. **2013** 13-21.

Su H, ZW, Guo J, Guo A, Yuan Q, Wu W. Neural progenitor cells enhance the survival and axonal regeneration of injured motoneurons after transplantation into the avulsed ventral horn of adult rats. Journal of Neurotrauma, **2009** 27, 67-80.

Takami T, Oudega M, Bethea JR, Wood PM, Kleitman N, Bunge MB. Methylprednisolone

and interleukin-10 reduce gray matter damage in the contused Fischer rat thoracic spinal cord but do not improve functional outcome. J Neurotrauma, **2002** 19, 653–666.

Tárnok K, Pataki A, Kovács J, Schlett K, Madarász E. Stage-dependent effects of cell-to-cell connections on in vitro induced neurogenesis. Eur J Cell Biol, **2002** 81, 403-12.

Terro F, Yardin C, Esclaire F, Ayer-Lelievre C, Hugon J. Mild kainate toxicity produces selective motoneuron death with marked activation of Ca(2+)-permeable AMPA/kainate receptors. Brain Res, **1998** 809, 319-24.

Tetzlaff W, Bisby MA, Kreutzberg GW. Changes in cytoskeletal proteins in the rat facial nucleus following axotomy. J Neurosci, **1988** 8, 3181-9.

Tran TA, McCoy MK, Sporn MB, Tansey MG. The synthetic triterpenoid CDDO-methyl ester modulates microglial activities, inhibits TNF production, and provides dopaminergic neuroprotection. J Neuroinflammation, **2008** 5, 1-14.

Trapp BD, Wujek JR, Criste GA, Jalabi W, Yin X, Kidd GJ, Stohlman S, Ransohoff R. Evidence for synaptic stripping by cortical microglia. Glia, **2007** 55, 360-8.

Vijayan VK, Lee YL, Eng LF. Increase in glial fibrillary acidic protein following neural trauma. Mol Chem Neuropathol, **1990** 13, 107-118.

Vise WM, Liss L, Yashon D, Hunt WE. Astrocytic processes: A route between vessels and neurons following blood-brain barrier injury. J Neuropathol Exp Neurol, **1975** 34, 324-334.

Walton NM, Sutter BM, Laywell ED, Levkoff LH, Kearns SM, Marshall GP, Scheffler, B, Steindler DA. Microglia instruct subventricular zone neurogenesis. Glia **2006** 54, 815–25.

Walz W. Role of astrocytes in the clearance of excess extracellular potassium. Neurochem Int, **2000** 36, 291-300.

Walz W, Wuttke W, Hertz L. Astrocytes in primary cultures: membrane potential characteristics reveal exclusive potassium conductance and potassium accumulator properties. Brain Res, **1984** 292, 367-374.

Wang J, Crawford K, Yuan M, Wang H, Gorry PR, Gabuzda D. Regulation of CC chemokine receptor 5 and CD4 expression and human immunodeficiency virus type 1 replication in human macrophages and microglia by T helper type 2 cytokines. J Infect Dis, **2002**,185, 885–97.

Wang XQ, Peng YP, Lu JH, Cao BB, Qiu YH. Neuroprotection of interleukin-6 against NMDA attack and its signal transduction by JAK and MAPK. Neurosci Lett **2009** 450, 122-6.

Zádori A, Agoston VA, Demeter K, Hádinger N, Várady L, Köhídi T, Göbl A, Nagy Z, Madarász E. Survival and differentiation of neuroectodermal cells with stem cell properties at different oxygen levels. Exp Neurol, **2011** 227, 136-48.

Zhang JY, Luo XG, Xian CJ, Liu ZH, Zhou XF. Endogenous BDNF is required for myelination and regeneration of injured sciatic nerve in rodents. Eur J Neurosci, **2000** 12, 4171-4180.

Zhou Z, Peng X, Insolera R, Fink DJ, Mata M. IL-10 promotes neuronal survival following spinal cord injury. Exp Neurol, **2009a** 220, 183-90.

Zhou Z, Peng X, Insolera R, Fink DJ, Mata M. Interleukin-10 provides direct trophic support to neurons. J Neurochem, **2009b** 110, 1617-27.

Appendix